UiT
NORGES
ARKTISKE
UNIVERSITET

Department of Engineering and Safety

Improving Mechanical Grip on Winter Tires

Finite Element Analysis on Pressure Profile of Airless Tire Compared to Conventional Tire Using ANSYS Workbench®

—

Sondre Ludvigsen

Master's Thesis in Technology and Safety in the High North – June 2017

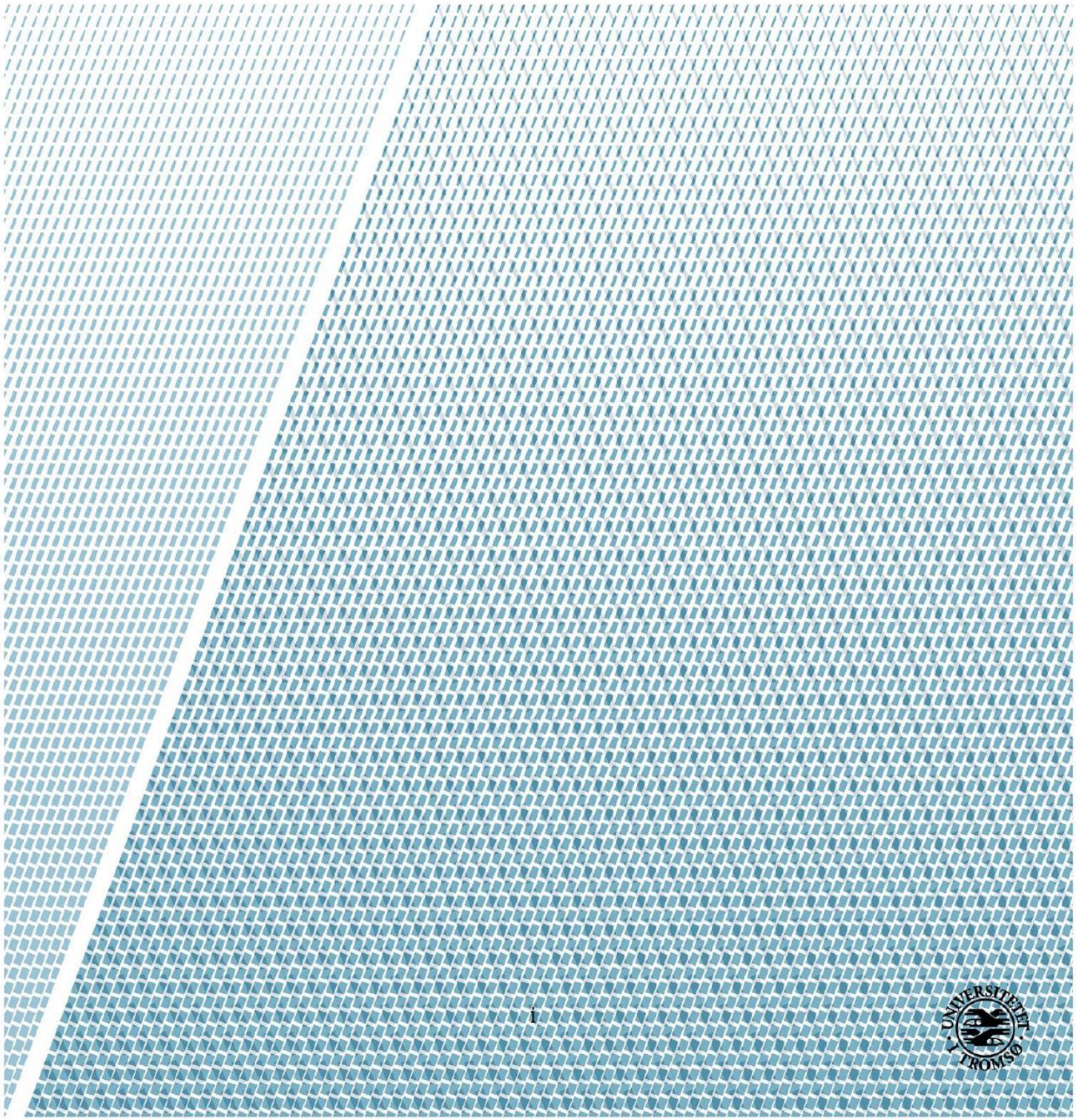

PREFACE

This Master's thesis is submitted as a fulfillment of my Master's degree Technology and Safety in the High North at UiT – The arctic university of Norway, Tromsø. The work in this thesis was carried out at the Department of Engineering and Safety in spring semester of 2017. It is the original and independent work of the author except where specifically acknowledged in the text. This Master's thesis contains 13990 words, 37 Figures and 8 tables.

Sondre Ludvigsen

Department of Engineering and Safety

UiT – the Arctic University of Norway

June 2017

ACKNOWLEDGEMENT

I want to acknowledge the professors and lecturers at the Department of Engineering and Safety for providing me with a good educational knowledge, preparing me for this Master's thesis. I want to give a special thanks to my supervisor, Dr. Hassan Abbas Khawaja for being available around the clock, for guidance on simulations and professional discussions on the literature.

Sondre Ludvigsen

Department of Engineering and Safety

UiT – the Arctic University of Norway

June 2017

ABSTRACT

The harsh climate of the arctic has always been one of the most difficult areas to drive cars in. The severe loss in traction due to snow and icing on the roads, has led to an increased risk of collisions. The winter tires for cars has developed through the years after their introduction in the 1930's. There have been three revolutionary changes made since then; implement of studs, changing in tread pattern and optimizing rubber characteristics. The implementation of studs is being shied away from today. This is a result of the ever-increasing focus on air pollution and environmental hazards, caused by the studs increase in road wear. It is believed that the tread design and rubber characteristics are close to their limit of further grip improvement, and thus the industry should look in new directions.

This Master's thesis purpose replacing the conventional air-filled tires with a non-air-filled tire to improve the grip in arctic conditions. The grip obtained for tires are determined by the weight of the car and the friction between the tire and the road. The friction coefficient, used to determine friction, is a function of the contact pressure. This thesis aims to obtain a concentrated pressure on the pressure profile for the airless tire, compared to a conventional tire. A finite element analysis, using ANSYS Workbench 18.0, is performed on two distinct models. The different pressure profiles of the models are analyzed and used for discussion on whether the airless tire has the potential of increased grip, under the same loading conditions as a conventional tire.

NOMENCLATURE

Table 1: Nomenclature

Symbol	Unit	Description
F	[N]	Force
R	[N]	Resistance due to friction
W	[N]	Force from the object to the surface below
N	[N]	Normal force from surface equaling the weight of the object
F_2	[N]	Compression or tension force on a spring
x	[m]	Displacement of a spring
k	[N/m]	Spring constant
E_P	[J]	Potential energy
E	[Pa] = [N/m^2]	Young's module
σ_1	[Pa] = [N/m^2]	Maximum shear stress in Von-Mises stress
σ_2	[Pa] = [N/m^2]	Medium shear stress in Von-Mises stress
σ_3	[Pa] = [N/m^2]	Minimum shear stress in Von-Mises stress
P	[Pa] = [N/m^2]	Inflation pressure
F_{MC}	[N]	Force from molecular collision
A	[m^2]	Surface area
F_{Car}	[N]	Force from car to the ground
F_{Wheel}	[N]	Force from one wheel to the ground
$A_{Rim\ surface\ area}$	[m^2]	Surface area of the rim
$W_{Width\ of\ rim}$	[m]	Width of the wheel
$D_{Diameter\ of\ rim}$	[m]	Diameter of rim
g	[m/s^2]	Earth gravity
P_{Rim}	[Pa] = [N/m^2]	Pressure in Y-direction on the rim

ABBREVIATION AND DEFINITIONS

Table 2: Abbreviations and definitions

Abbreviation	**Explanation**
FEA	Finite Element Analysis
FEM	Finite Element Method

LIST OF CONTENT

LIST OF FIGURES

LIST OF TABLES

1 INTRODUCTION

This thesis aims to improve the grip of vehicular winter tires by performing a Finite Element Analysis on a pneumatic and a non-pneumatic tire model. Topic included are how the industry today are working on improving their winter tires and how other companies have looked at different concepts of airless tires. Lastly the Finite Element Analysis are presented with respect to design, analysis approach and results.

1.1 EVOLUTION OF WINTER TIRES

The first winter tires used for road cars where applied during the mid-1930's. The difference to these tires compared to the summer tires, were the enlargement of the grooves. Deeper lateral groves gave better traction as it allowed the tread blocks to dig deeper into the snow-covered roads. In 1961 the first tires with metal studs were introduced. The studs help the tire gaining grip on hard packed snow and ice as the studs claws into the ice and increases friction. The focus the last 50 years have been on improving traction by optimizing rubber compositions and treading. This can be done by changing parameters like elasticity, hardness, adding of studs as well as modifying tread pattern design. In summary, there have only been three major innovations to improve the winter tires since their arrival 80 years ago; Changing the treading, adding metal studs and optimizing rubber composition. In recent years the government and manufacturers have been looking towards stud-free winter tires due to environmental benefits. By now removing one of the three breakthroughs in the evolution of winter tires, there is a limit on how much you can improve today's pneumatic winter tires without thinking in new directions! [1]

1.2 COMMON DEFINITION OF GRIP

Before looking in depth at the tire, we explain how the common perception of grip is. To explain what grip is we look at what situations, and how the term is being used in everyday situations. The general perception of having good grip, is when two objects with forces parallel to their contact area, don't move relative to each other. In other words, grip is the force or contact that gives us the ability to stay in contact with surfaces without slipping, referred to as frictional force. We differentiate grip in three categories; no grip, sliding, and sticking. No grip means no resistance against movement thru zero frictional force. In real life, this is impossible to achieve as there will always be some energy transfer between moving objects, often in form of heat accumulation. Sliding friction is having a sliding motion but with friction working against the direction of travel. This friction force will limit the velocity by transferring the kinetic energy into potential energy, in form of heating generation on the contact surface and the object. Sticking grip is where you have enough frictional force to prevent any movement between the two objects. This means, from a stationary position that the frictional force is greater than the force trying to move the object.

We can use an example with pushing a box, to illustrate grip and its physics better. The box has sticking grip when it can't be pushed, and has limited or loss of grip when it can be moved by pushing or pulling. We can now have a closer look at what causes the box to be able to move. The reason for this to happen is that the pushing force exceeds friction force between the box and the ground. This friction force is the two surfaces resistance for relative motion, which can be in form of rolling or in this case sliding. By having high friction, high resistance against sliding, we have good grip. In figure 1 the friction force (R) exceeds the pulling force (F) and hence, the box would not move.

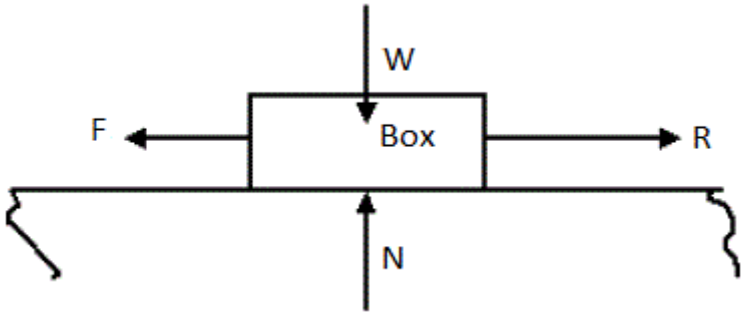

Figure 1: Friction force on a box with applied force [2]

There are two factors that changes the level of friction; surface friction coefficient and normal force (N). This is seen in the friction formula (1)

$$f_{Friction} = \mu_{Friction\ coefficient} \cdot N_{Normal\ force} \quad (1)$$

The surface friction coefficient is the surfaces gripping ability against each other. For example, a soft rubber piece has a higher friction coefficient against a metal plate than a metal on metal contact has. To implement this in the example with the box, we would have a higher friction coefficient if the contact surface is dry, compared to a lower friction coefficient if it was covered in grease or another slippery fluid. The other parameter for increasing grip is increasing the normal force (N). the normal force is counteracting the weight of the box. If the object sits on a level surface, the normal force would be equal to the weight working perpendicular to the objects contact area. If a force applied on the side of the box is making it move, you can apply a higher normal force by adding more weight to the box. By doing this you increase the friction force between the box and the ground, and again, by increasing the friction force we increase the boxes' resistance for relative motion. In this thesis however, the objective is not to improve grip by increasing the weight of the car or change the materials. As $\mu_{Friction\ coefficient}$ is a function of pressure, having a pressure concentration will lead to a higher $\mu_{Friction\ coefficient}$. The aim of the Thesis is thus to increase the value of $\mu_{Friction\ coefficient}$, by having a more concentrated pressure on the pressure profile between the two objects. In this case the pneumatic model pressing on the ground compared to the airless model pressing on the ground with equal force. [3]

1.3 Grip in This Paper

With the knowledge about the definition of grip, we can look how this project presents a way of increasing grip of a winter tire. The aim is, as mentioned, to change the contact pressure profile between the tire and the ground. As a conventional pneumatic tire contains pressurized air, this pressure is always uniformly distributed throughout the inside of the tire. This will give it a more uniformly distributed contact pressure profile. We are trying to change this pressure profile by concentrating the pressure from the tire down to the contact area. The theory is that this is possible by replacing the pressurized air with springs. This thesis performs a Finite Element Analysis (FEA) to see if this theory can be proven. More details on the physics comes in chapter 2.

1.4 Winter's Effect on Driving Physics

Winter conditions makes the challenges of driving significantly harder and more unpredictable. Although there are less fatalities from traffic accidents during the winter compared to the summer months [4], there are a higher total number of accidents during winter, like low velocity collisions. The loss of friction between the road surface and tire, reduces the grip of the car. This weakens the car's ability to accelerate, meaning a change of velocity in any direction such as turning, braking and accelerating forward. There are other characters of winter effects that causes loss of friction, like the added danger of hydroplaning or the temperature's effect on the rubber behavior.

1.5 Studs Damaging the Roads

Implementation of studs in the winter tires helps improve traction. This is true as the metal studs has a high-pressure concentration due to its small surface area, making it able to penetrate the ice surface. While the implementation of studs is a great way to improve the friction between the tire and the icy road surface, it has its drawbacks. The government and environmentalists advise us to choose stud-free winter tires as the negative effects of studs are more known and gaining more attention today. Environmentalists worries about the increase of particulate matter, polluting the air we are breathing in, which is especially bothersome for asthmatics [5]. The reason for increased pollution with studs are due to the increase the abrasive wear on the roads (figure 2). The studs are carving of small particles of the asphalt, which are mixed in with the air we breathe in. This will of course happen without the studs as well, but the amount of particulate matter pollution increases as the studs provides more abrasive wear than stud-less tires [6]. The government are, in addition to people's health, interested in the way studded tires impose a threat to the condition of the road. As the season changes and temperatures vary, the ice is being melted or scraped off the road surface by the many vehicles driving. This in addition to the increasing use of road salt, which reduce the ice accumulation on the roads, leaves the asphalt exposed to the studded tires which erode the asphalt. This has brought an increase on the expenses of road maintenance as it is forcing shorter maintenance intervals due to the increased wear [7]. These are some of the motivators

for going away from studded tires, and a part of this thesis's motivation for improving the non-studded tires effectiveness.

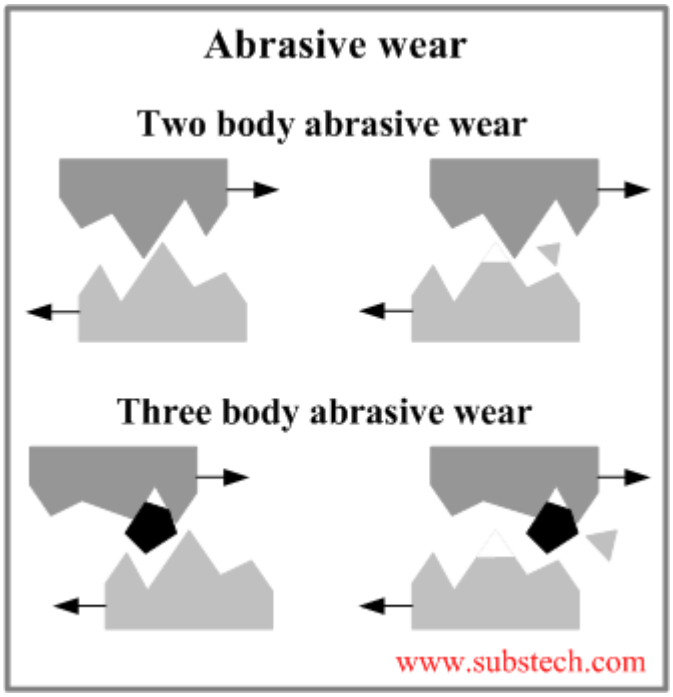

Figure 2: Illustration of abrasive wear [8]

2 LITERATURE REVIEW

This chapter discusses the literature involving both pneumatic and non-pneumatic tires, and the theory and physics behind them.

2.1 TIRE ANATOMY

All conventional car tires have a common ground baseline on how they are built up across the different tire manufacturing companies. Every company must overcome the same challenges when designing a winter tire. The tires are supposed to have a compromise between being best suitable of maintaining a sufficient level grip on the road, while giving the car a safe, predictable and enjoyable ride. Beyond this, the tire can be constructed to have different abilities such as longevity, low rolling resistance, low sound emitting or maximum grip under given circumstances. Consumers are generally interested in having a decent combination of all mentioned attributes.

This chapter presents how a tire is built up (see figure 3), and what challenges each component cope with. The different components have their own benefits, but also works together on providing some tire characters like e.g. providing strength to ensure the tire's structure is maintained under stress and strain.

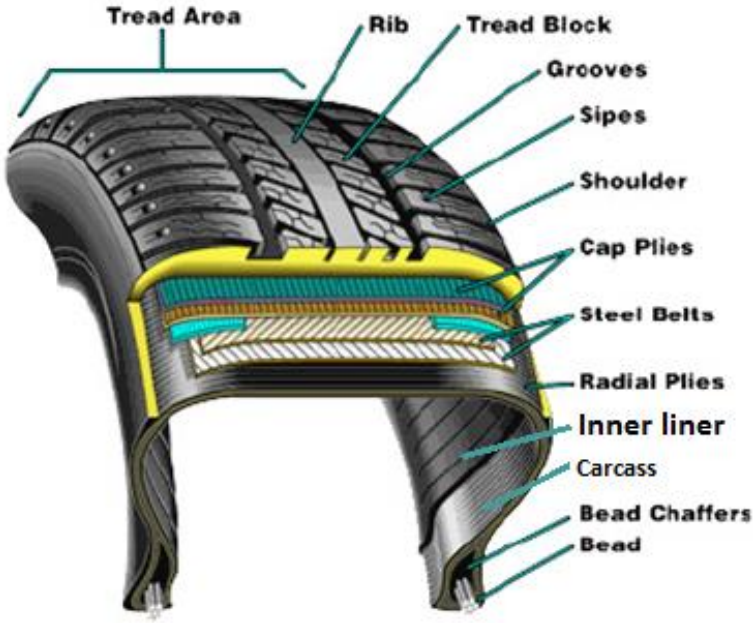

Figure 3: A tire's anatomy [9]

2.1.1 Tire Components

The components of the tire listed below can be also be seen graphically in figure 3

Inner liner:

- The first material from the inside is a synthetic rubber providing an air tight layer. This is to prevent any leakage of air which would lead to a pressure loss inside the tire.

Carcass

- The carcass is made with strong textile fiber cords implemented in a rubber housing which objective is to maintain the tire's shape under internal pressure. This ensures that the tire won't bulge out when inflating it.

Beads:

- The beads are steel wires included in the part of the tire sidewall in contact with the rim. The purpose of the wires is to ensure an airtight contact so the tire pressure won't drop due to an air leakage between the tire and the rim. These wires are strong. A set of wires included in the tire can in some tires withstand ten times the weight of the car.

Sidewalls

- The sidewall is where the logo of the manufacturer and the details about the tire and its production is printed. The details are preferably; dimensions of the tire, speed rating, preferred rolling direction and the month and year of when it was produced.

Steel belts

- Steel belts are bounded into the rubber providing strength. This makes the tire's ability to handle the strain from turning and preventing the tire to expand from the centrifugal force caused by fast rotation.

Cap plies

- The cap plies are rubber layers with integrated nylon that stretches around the circumference of the tire, located between the steel belts and the treading. This layer both adds resistance against expansion and reduce heating induced by friction.

Tread

- The tread is the part of the tire in contact with the road and is the visible part of the tire. This is the part of the tire that in the highest degree determines quality and characteristics of the tire performance. The objective of the tread is to provide grip against the road surface while providing a low level of abrasion and heat generation. Each manufactory uses their own material composition and tread pattern that based on what their calculations and testing says is the best solution for given conditions. More on the treading and material in chapter 2.1.3 – "Winter tire vs summer tire"
- Grooves are the cuts in the tread making the tread patterns. The treading is responsible for road noise mitigation, water diverting, and to provide a large contact area with a

correct frictional coefficient to provide sufficient grip in given temperatures and conditions.

2.1.2 The Manufacturing Process of a Tire

The tire is generally made in three steps by three different machines. The first mixes the rubber compound, the second one applies the correct materials at the correct locations, while the third defines the final shape, tread pattern and vulcanizes the rubber.

The first stage of making a tire starts with mixing the different rubber types, which can be around 30 to 40 different types. The mixture is then added with oil, pigments and other chemical additives. A large blender with high temperature and pressure, mixes all the materials into a soft rubber compound. This compound is then sent to different processes to be made into other parts of the tire like sidewalls, inner liner, carcass etc.

To apply each component to the tire, a special metal cylinder with a flexible inflatable middle is used. Each layer of tire component is rolled onto this drum starting from the inner parts working its way outwards. The components are applied in the order that they are presented in chapter 2.1.1, starting with the airtight inner liner and ending with the sidewalls.

The middle part of the drum which these materials are wrapped around, expands. This procedure is shaping the tire approximately to its final form giving the sidewall and contact area a visible dividing. Now the cap plies and steel belts layer can be added on top before finishing with the tread material layer.

After all the materials have been added, the tire is placed in the third machine, the curing mold. On the inside of the mold, the tread pattern and law regulated sidewall prints are engraved. Hot pressurized water is then applied inside of the tire, pushing the rubber into the grooves of the mold, forming the tire. The heat from the steam and water starts the curing and vulcanization of the rubber, at a temperature of around 300 degrees. The vulcanization makes the rubber go from its sticky plastic deformation state (when deformed the rubber stays in its new shape), to have elastic deformation characteristics, (when the rubber returns to its initial state when applied strain stops). [10]

2.1.3 Winter Tire vs. Summer Tire.

A test performed by Auto Express in 2011 showed a huge improvement in cold climate performance of a stud free winter tire compared to a summer tire. They conducted the test with two cars of the same make and same tire manufacturer, in subzero temperatures on snow packed ice. The test was measuring braking distance when going from 48 km/h to zero. The winter tires stopped after 27 meters compared to the summer tire’s 85 meters. This is a massive difference and shows the importance and advantage of a winter tire over a summer tire in arctic conditions. [11].

2.1.3.1 Treading Differences

There are some key differences to a winter tire compared to a summer tire other than the possible addition of studs. The most noticeable being the shape and pattern of the treading. As figure 4 shows, the summer tire (a) has large tread blocks divided by wide grooves. These groves are mainly oriented in the longitudinal direction (rolling direction) for maximum water displacement at higher speeds. The tread blocks are also smooth on the top for maximum contact area.

Figure 4: Comparison of summer tire (a) vs winter tire (b). [12]

The winter tire's treading, seen as (b) on figure 4, is very different to the treading of the summer tire. The winter tire has more, but narrower grooves. The grooves are a little deeper than on winter tires, and oriented in different directions including lateral direction (perpendicular to the rolling direction). This makes for an efficient deflection of water and slushy snow, providing the tread a better contact with the road without hydroplaning. This is more crucial in arctic condition due to more exposure of water. As the tire is compressing the snow, this pressure gives a local increase in temperature, hence melting the snow to a water film on the contact layer between the road and tire. This water needs to be moved from underneath the tread surface to prevent hydroplaning, and is effectively done so by the unique tread patterns of winter tires.

Figure 5: Winter tire packed with snow [13]

Figure 5 shows a winter tire with packed snow, both in between and on the tread blocks. In first sight, it might be tempting to remove this snow before going on a drive. That is not recommended as the tread is designed to keep the snow like this, as it helps grip on snow packed roads. This is because snow on snow traction is very good. An example of good snow on snow traction is known from building a snowman or an igloo with compact snow.

The winter tire also has these very narrow cuts on the top of the tread blocks, called sipes (also seen in figure 3). These provides more biting edges on the contact area for the tread to grip and hold onto the snow, like seen in figure 5. By having sipes, the tread blocks are also more capable to dig in with the irregularities of the road rather than having a totally flat surface, relying on the rubber softness to be able to deform into the irregularities for grip. The sipes are often oriented in different directions over the width of the tire, or formed in zig zags. This helps by having biting edges in both longitudinal and lateral direction providing grip in both directions. [14], [15]

2.1.3.2 Rubber Characteristics and Compound

The rubber composition is softer on winter tires than summer tires when compared in the same temperature. This is because each compound is designed to work optimally in a specific temperature range. When the temperature decreases below a certain value, defined by the compound, the rubber reach glass transition temperature. What happens below this temperature is that the rubber hardens as the molecules moves less freely. This causes a decrease in friction coefficient which gives the tire less grip on the road, and is one of main reasons why summer tires work poorly in cold winter conditions. A softer winter tire can deform to match with the road better compared to the hard summer tires that are likely to rest on top of the small imperfections of the road. Each compound has its own glass transition temperature, which of course is lower for winter tires compared to summer tires. It's generally recommended to use winter tires in temperatures below 7 degrees Celsius due to this difference of rubber characteristics in low temperatures.

The tire compound from some winter tire manufacturers also includes pores throughout the full thickness of the tire. These pores soak up the water film created on the road surface due to the sun or contact pressure melting the snow. By having these pores soaking up the water the tread has a cleaner contact with the road, providing less chance of hydroplaning and more grip. Two pictures taken from a demonstration video made by Bridgestone Tires, shows how these pores works (Figure 6).

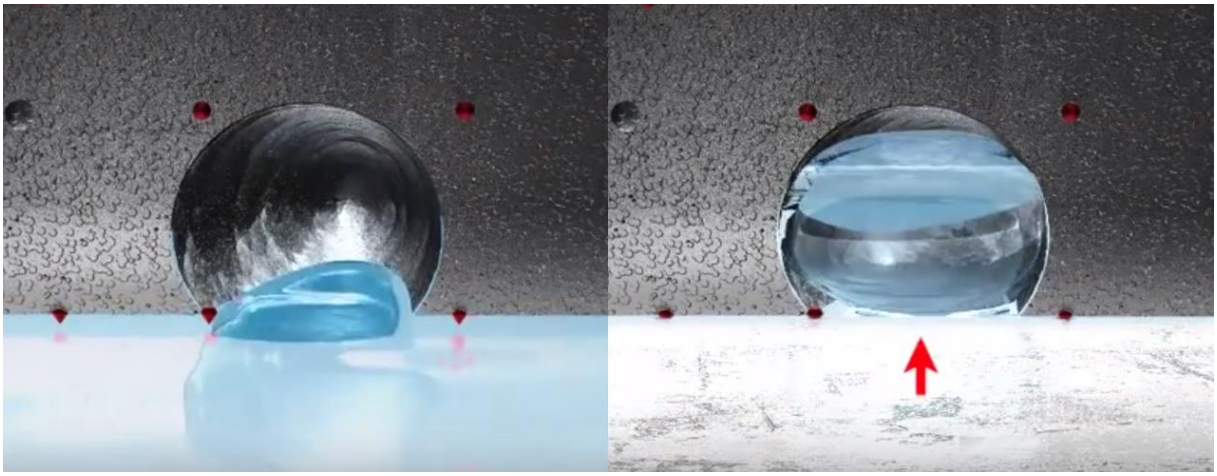

Figure 6: Pores in tire removing water film [16]

2.2 ANSYS WORKBENCH

For the simulations done in this thesis, ANSYS Workbench version 18.0 was used. ANSYS Workbench is a powerful software tool to help solve complex engineering tasks. This program can simulate various Multiphysics problems, like heat diffusion, stress and strain analysis, fluid mechanics and more, and gives accurate and reliable results based on the quality of the inputs. ANSYS is an acknowledged software and is used by many big companies with different areas of expertise. One example is that Ferrari used it for aerodynamic studies, to save several hours of expensive wind tunnel testing in the process of designing their hyper car, Ferrari Laferrari. This is a proof of how accurate and appreciated software programs like ANSYS Workbench are in the industry today. [17]

2.3 FINITE ELEMENT METHOD (FEM)

For analyzing the contact pressure profile in this thesis, ANSYS Workbench's feature, static structural analysis was used. This analysis uses the finite element method. The finite element method is based on dividing a complex structure into a finite number of smaller elements. By knowing the behavior of some of the elements, the behavior of the complete structure can be found by assembling these elements. To find the numerical solution, using FEM, a set of mathematical formulas are solved simultaneously. These formulas are related to each node made from dividing the structure into smaller elements. Each element has a certain number of nodes connected to it. The element shape with the lowest number of nodes are triangular element with 3 nodes, one in each corner. The simplest quadrilateral has a node in each of its four corners when looking at a 2D element. This can also be expanded to for example an eight-node quadrilateral by having nodes in the center of the lines connecting each corner. This is however, most used in very complex shaped structures.

The way that the finite element method works is that each node can move from its original position when applied a load. Each node has 6 degrees of freedom and can move in both X,Y and Z direction as well as rotate around these 3 axis. As the elements are connected to each other by nodes, and each node has its set of equations, a load applied to one side of the structure will transfer through the structure via the element nodes.

The divided structure makes a mesh of elements. The number of elements are decided by altering the mesh density. The finer the mesh density, the more elements we have hence more accurate results can be acquired. A converging study should always be considered to validate the results. Another benefit of a mesh study is to recognize if the mesh has a too fine density. Using a finer mesh density is very demanding of computational power, as the results are based on simultaneously solving the equations for each node. Hence why a mesh density should give accurate results, but not be unnecessarily demanding of computational power.

2.4 Static Structural Analysis

ANSYS Workbench's static structural analysis has Hooke's law as the main formula behind the calculations with both linear materials and non-linear materials. A linear behavior is when the displacement and force is directly proportionated to each other. This contrasts with a nonlinear behavior where the stiffness changes depending on the force. Hooke's law is presented as formula 3 below where F_2 is the force, x is displacement and k is the spring constant. With non-linear behavior, the k is no longer linear but changes as a function of displacement. Some assumptions made in the presented formulas below is that the material has linear elastic behavior, forces are not time varying and there are no inertial effects like dampening included. [18]

$$F_2 = kx \tag{3}$$

Where:

$$k = \frac{\Delta F_2}{\Delta x} \tag{4}$$

If we integrate Hooke's law we get the formula for potential energy, below in formula 5.

$$E_P = \frac{1}{2}kx^2 \tag{5}$$

To perform a static structural analysis some material properties are required. Two of the following four properties is needed; Young's modulus, Poisson's ratio, Bulk modulus or shear modulus. The most common to use, and the one listed in this thesis, are the Young's modulus and the Poisson's ratio. However, ANSYS Workbench can by knowing two of these parameters provide the values for the two unknowns. The Young's modulus, also referred to as elastic modulus, is a value to describe the elastic properties of a material under pressure or tension. A high Young's modulus means that the material has a high resistance against deformation under loading. The unit is Pascals, and that is newtons per square meter (N/m^2) with the SI-units. The Poisson's ratio tells how much lateral strain the material is having under compression or tension, and is dimensionless. [19]

2.5 Equivalent Stress in ANSYS Workbench

The equivalent stress tool in ANSYS Workbench is a handy tool that allows three dimensional stresses to be displayed in one positive stress value, often presented on the model in color contouring. The equivalent stress, or von Mises stress as it's also called, is calculated from formula (6).

$$\sigma_e = \left[\frac{(\sigma_1-\sigma_2)^2+(\sigma_2-\sigma_3)^2+(\sigma_3-\sigma_1)^2}{2}\right]^{\frac{1}{2}} \quad (6)$$

The sigmas in the formula are called principal stresses. These are derived from the plasticity theory, saying that "an infinitesimal volume of material at an arbitrary point on or inside the solid body can be rotated such that only normal stresses remain and all shear stresses are zero" [20]. Where σ_1 is maximum stress, σ_2 is middle stress, and σ_3 is minimum stress. To be used in formula (6) these principle stresses are always ordered like $\sigma_1 > \sigma_2 > \sigma_3$. The equivalent stress can be expanded to include in the maximum equivalent stress failure theory. This is often related to as von Mises yield stress criterion and can be used to predict the yield point, or maximum yield stress, for a ductile material. A ductile material is a material that deforms under tensile load unable to return to its initial shape, also called plastic deformation. [20]

2.6 Physics of Pressure Profile

When pressurizing air, the pressure is distributed uniformly over the inner surface area of the volume, for example a tire. This is achieved as the air molecules are moving freely inside the volume, bouncing into each other and the inner surface of the tire. These small collisions that happens an uncountable amount of times per second is too small to be measured. There are so many collisions that they make it to appear as the inner surface is under a measurable constant pressure acting perpendicular to the surface area. Formula (7) shows how pressure is dependent on the force (F_{MC}) and the surface area (A). F_{MC} is determined by the number of collisions between the molecules and the surface area of the tire wall (A). So, by bringing more air molecules into the tire, by inflating it with air, we have more collisions and hence an increase of pressure inside the tire.

$$P = \frac{F_{MC}}{A} \quad (7)$$

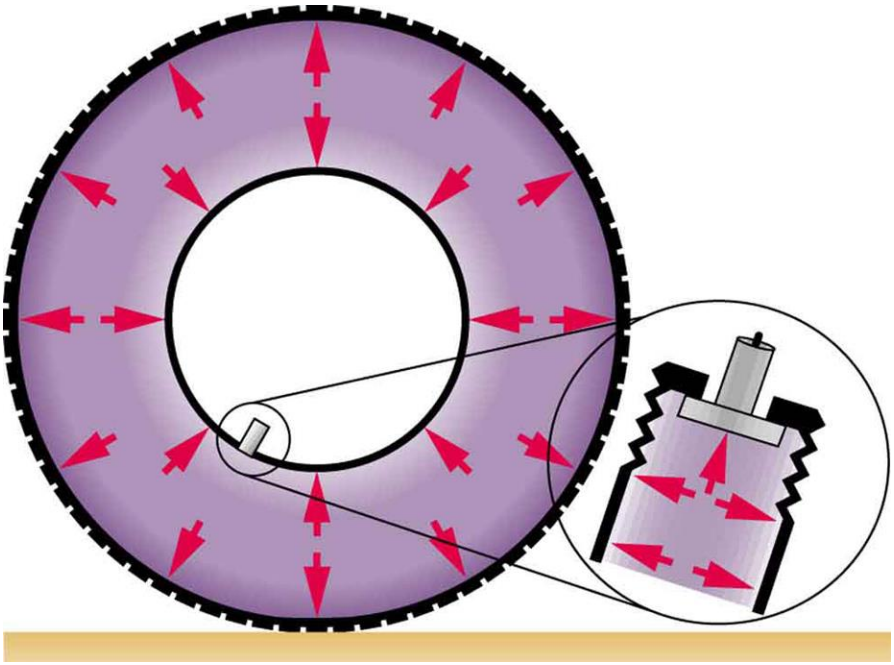

Figure 7: Illustration of uniformly distributed tire pressure [21]

With this being known the pressure inside a car tire can be illustrated like in figure 7. Where pressure on every part of the surface area is equal and acting perpendicular. So even with a deformation of the tire due to it being pushed on the ground, the pressure is still equal throughout its inner surface. This behavior is likely to give an equal uniform pressure profile over the contact area with the ground. Some variations can occur due to the inflation pressure values as seen in figure 8. A drawback of using pressurized air inside the tires, especially in arctic conditions, is that the pressure of the air is temperature dependent. If the temperature decreases by 1 degrees Celsius, the pressure drops by 0,19 PSI or 0,013 bars. If the temperature fluctuates by 20 degrees the pressure will change by 0,26 bars, which dependent on initial pressure can bring the tire to an under-inflation state. This temperature effect can, by changing to a non-pneumatic tire with suitable spring materials, be small enough to be neglected.

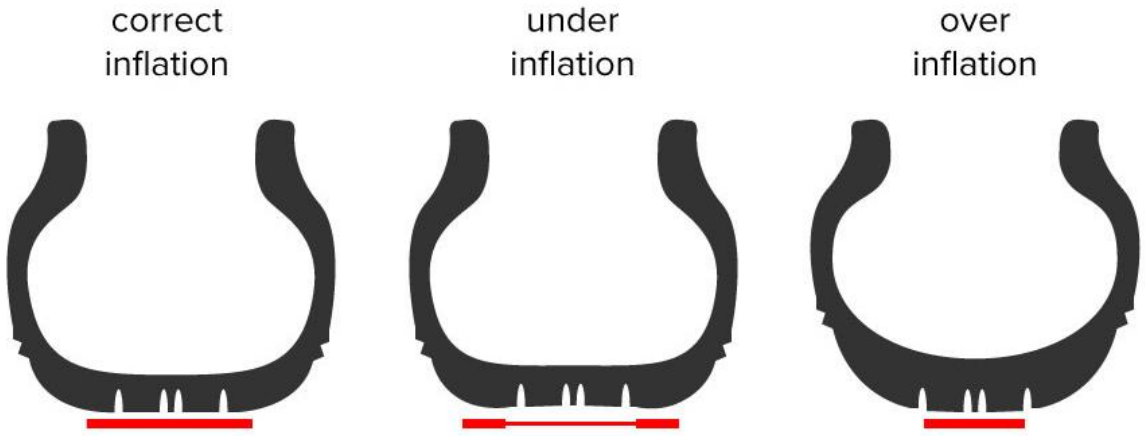

Figure 8: Illustration of tire pressure changing the contact area [22]

2.6.1 Non-Pneumatic Contact Profile Theory

The pressure profile from a non-pneumatic tire might not be the same as for pneumatic tire as we have springs transferring the weight of the car to the ground instead of air. We can look at figure 9 showing an exaggerated picture of a non-pneumatic tire being pushed down into the ground, where the red lines are symbolizing the tire springs closest to the contact area. As Hooke's law explains (formula (3), the force on a spring with linear behavior (constant spring constant) is determined by the displacement. This means that the springs that are being compressed the most will have a higher force. The force from these springs are passing thru the rubber and down to the ground, influencing the contact pressure between the tread and the road. The spring being compressed the most, in a stationary situation, is always the one in the middle. The theory is that this is going to produce a higher pressure consecration in the middle of the contact pressure profile.

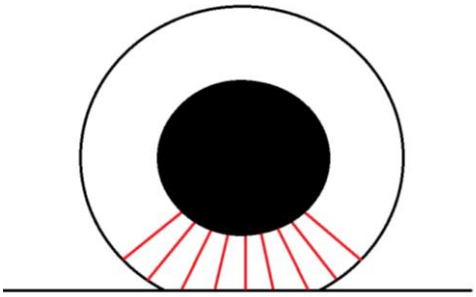

Figure 9: Illustration of the springs in a non-pneumatic tire being compressed against the road

2.7 Other Concepts of Airless Tires

There have been companies doing studies on airless tires both in the past and present. In this chapter, we are presenting some of the concepts. None of the models have been reported tested for arctic conditions.

2.7.1 Tweel

One of the best proven concepts so far of airless tire for everyday use, is the Tweel made by the French tire company Michelin. The project started in 2005 and was ready for first productional delivery in 2013. This design won several awards for its design and creative thinking. As figure 10 shows, the most noticeable difference is that the air in pneumatic radial tires are replaced with strong poly-urethane spokes. These acts like shock absorbers and holds the weight of the car. The outer part is made of reinforced steel band to make for a good contact patch to the road surface. A layer of rubber is added outside for friction against the road. Michelin especially highlighted the benefit of never having to replace a deflated pneumatic tire, and that replacing the rubber of the Tweel is much easier and cheaper. [23]

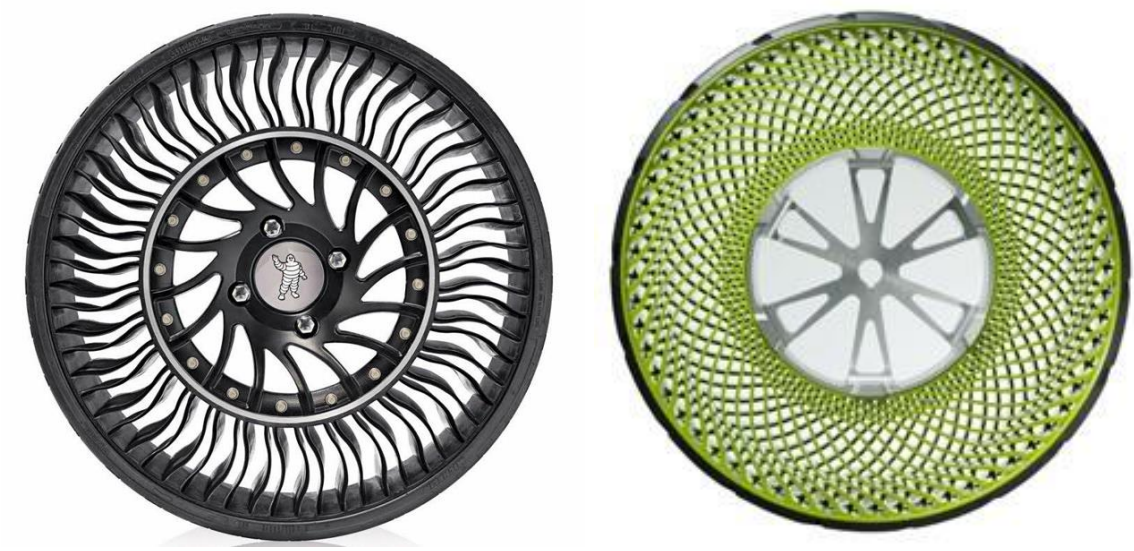

Figure 10: Michelin's Tweel (left) and Bridgestone's airless tyres (right) [24] [25]

Today the Tweel is mostly used on slow moving vehicles, like constructional vehicles and lawn mowers. Michelin claims that the Tweel reduces the bouncing motion you often get with pneumatic tires on wheel loaders and other small diggers. There are a few reasons for why the Tweel is only used on slow paced vehicles and not on road cars. Conservative road regulations being one of them. Michelin also reported some challenges at high speeds of, high temperature generation, slight high values of noise and vibration. These are also the main drawbacks of the particular design of the Michelin Tweel to date. [26]

As the wheel is made non-pneumatical the engineers have more freedom to come up with design specifically for its intended task and operational environment. As we have springs or blades, you can alter the shape or angle to make for the characteristics you aim for, like

stiffness in lateral or longitudinal direction. This can be a benefit over the conventional pneumatic tire, that has the disadvantage of the sidewall bending at high lateral stresses. With this design, you can almost completely remove this behavior if wanted. [27]

2.7.2 Lunar Tires

The Lunar tires, displayed in figure 8, are the wheels used on vehicles operating in space. The Lunar Tires are in many ways similar to the Michelin Tweel in terms of thinking and design philosophy. The Lunar tires has replaced the air within the tire with springs and shock absorbers. It also replaced the rubber contact area with a pattern of steel plates attached to the meshed contact surface, for better traction on the moon's uneven surface. There are several benefits from this design. By removing the air, you remove the possibility of having a flat tire, which would be catastrophic on the moon. Another benefit is the increased mechanical grip, as the wheel is more able to shape around objects to compensate for the decrease in gravity. [28]

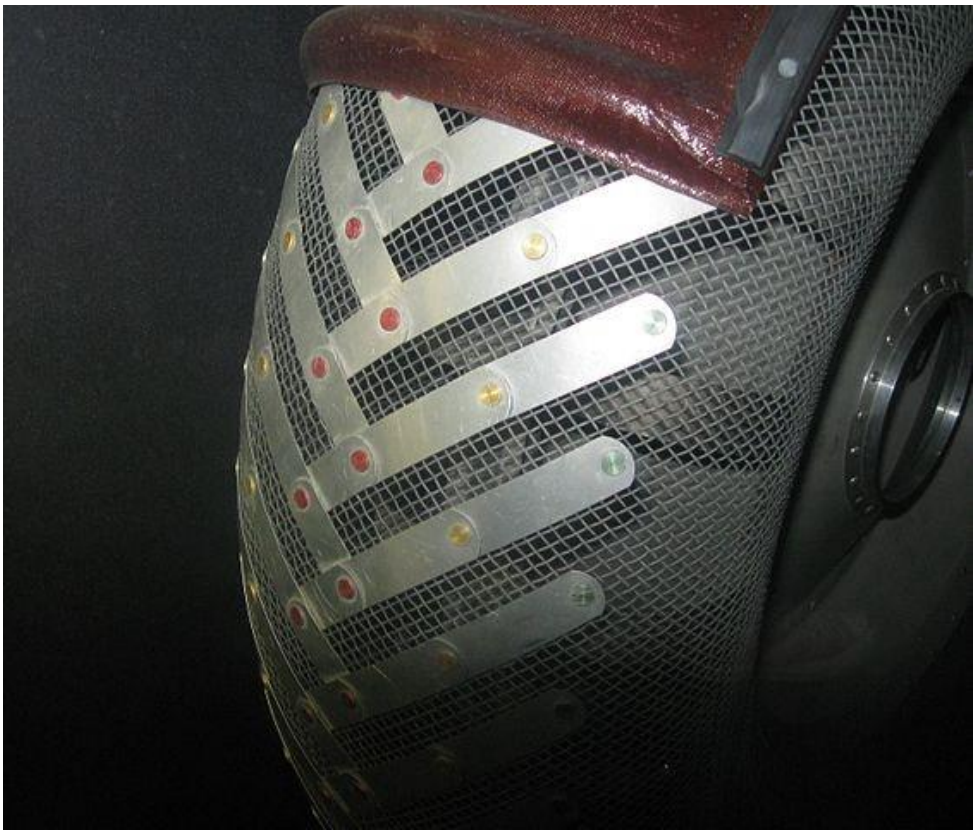

Figure 11: Lunar tire [28]

3 METHODOLOGY

In this chapter, the models and the thoughts behind them and their design are presented. As well as explaining a about the FEM analysis approach on ANSYS workbench version 18.0.

3.1 PRELIMINARY STUDY

A preliminary study was done before this master thesis, performed in ANSYS Workbench version 16.2. This study aimed to ensure that improving mechanical grip by using airless tires were possible. Like this thesis, the results of two models were compared.

3.1.1 Model and Geometry

There were two models in this study, one pneumatic and one non-pneumatic. Both with the same dimensions of a 205/55/R16 tire, to have comparable results. When decoding the tire size number we have the dimensions as presented in table 3.

Model	Tire width [mm]	Height of tire wall [mm]	Rim diameter [mm]	Thickness of rubber [mm]	Surface area of rim [m^2]
Pneumatic tire	205	113	406	20	0,255
Non-pneumatic tire	205	0	500	20	0,314

Table 3: Dimensions used in preliminary study

The models were made in ANSYS Workbench and were simplified tire models. The pneumatic tire model (figure 12), contained 4 bodies; the ground block, rim, tire, and a suppressed body taking the volume of air (highlighted green in figure 12). The rim was made by having a solid cylinder in the center.

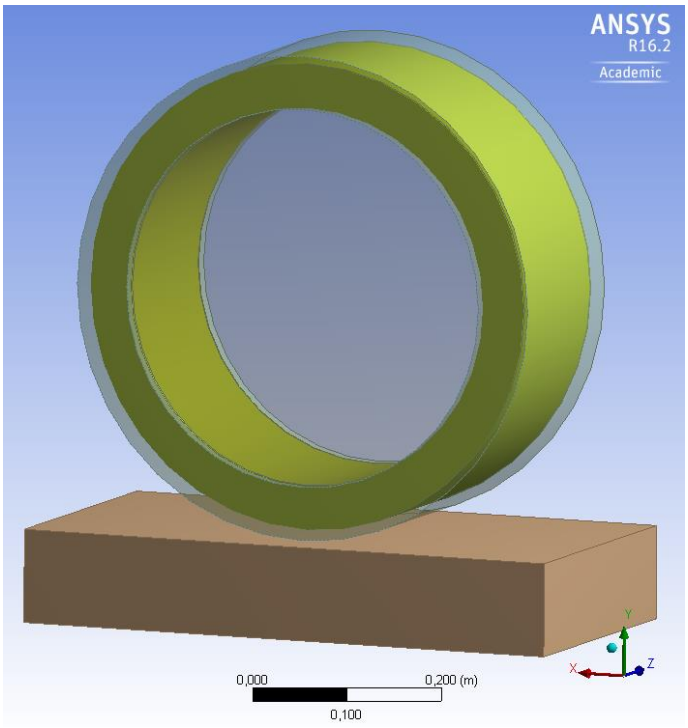

Figure 12: Pneumatic tire model from preliminary study

The non-pneumatic tire (figure 13) was made similar to the pneumatic tire. However, being airless it had 3 bodies. A wider rim cylinder replaced the air's volume, still having the same outer dimensions as the pneumatic model. A 20 mm rubber stretched around the cylinder's circumference made for a contact area with friction.

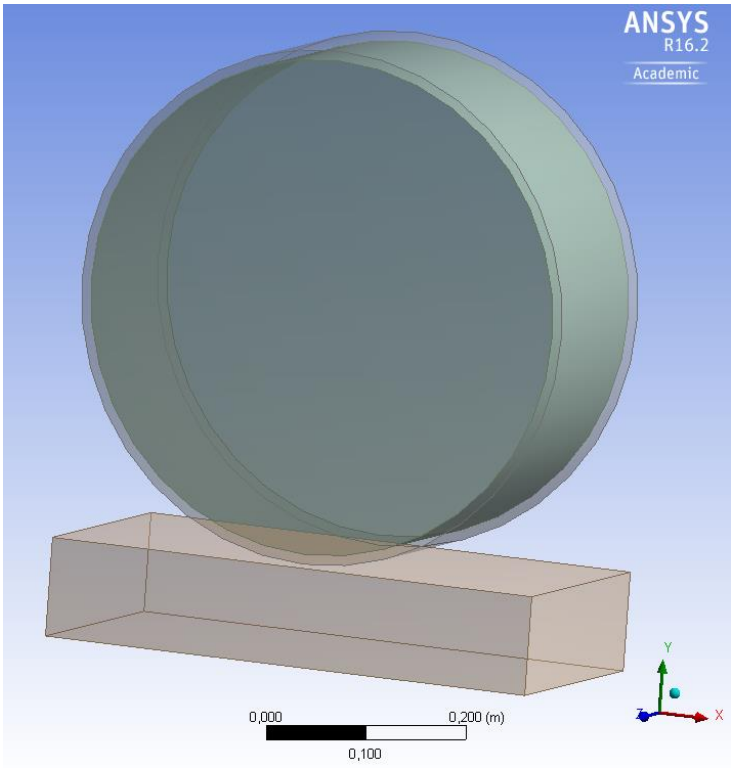

Figure 13: Non-pneumatic tire model from preliminary study

3.1.2 Materials in Preliminary Study

The materials for this study were both taken from the ANSYS Workbench library and custom made. The material for the block under the tire and the rim, were selected from the library to be concrete and structural steel. As chapter 2.1 - tire anatomy explains, a tire can consist of tens of different materials variations and rubber compounds. This was simplified by making a custom rubber compound to combine all the components characters into one material. The material properties of this custom rubber, and other materials used, is presented in table 4.

Material	Density [Kg/m^3]	Young's module [Pa]	Poisson ratio	Area used
Concrete	2300	3 E+10	0,18	Ground
Structural steel	7850	2 E+11	0,3	Rim
Custom rubber	650	5 E+7	0,47	Tire against ground

Table 4: Materials used in preliminary study

3.1.3 Meshing in Preliminary Study

Figure 14 shows the mesh of the two models in this study. The meshing of the groundt block was ensured to be of quadrilaterals for both models as the mesh density were limited by the license. This made them more comparable when looking at the frictional contact profile and contact pressure profile in the results.

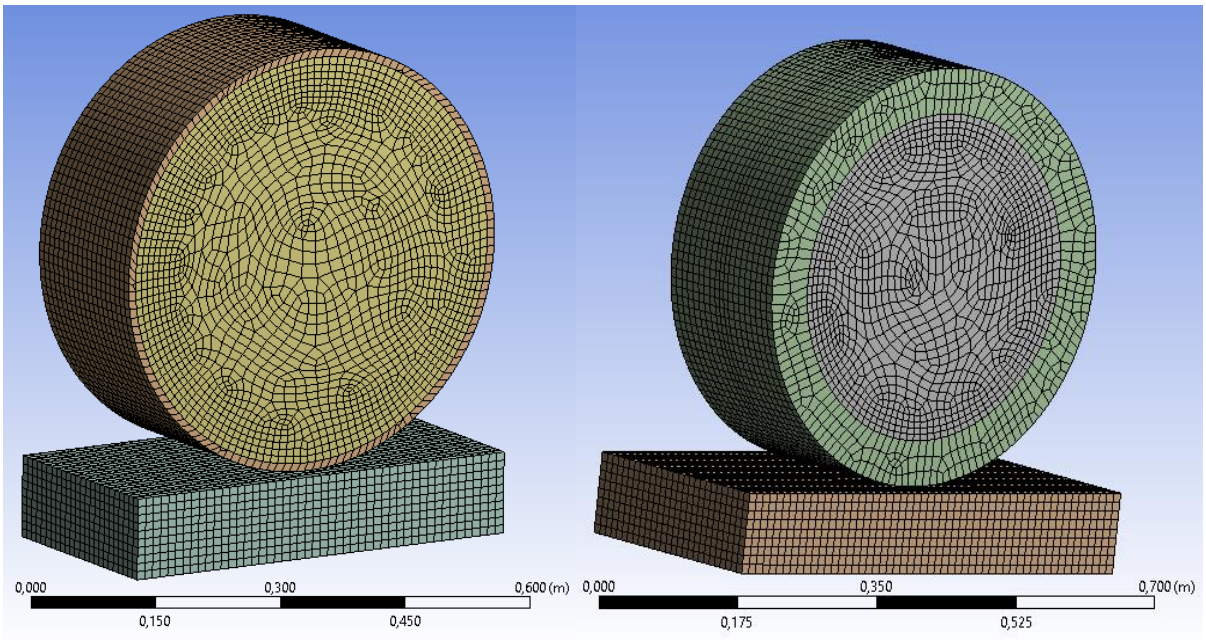

Figure 14: meshing of the two models from preliminary study

The non-pneumatic model on the left, had a total of 217927 nodes and 48399 elements. The pneumatic model on the right had a total of 215802 nodes and 55168 elements. A finer mesh was tried but the student license in ANSYS Workbench were limited. However, for a preliminary study it was assumed to be a sufficient mesh density.

3.1.4 Calculation of Forces in Preliminary Study

For the simulations, the mass of the car to 1500 kg, which is around the average weight of a car. The calculations below show how this weight was used to get the correct pressure applied to both models.

Force from the car (F_{Car}) calculated by multiplying the weight (W_{Car}) by gravity (g)

$$F_{Car} = W_{Car} \cdot g \tag{8}$$

$$F_{Car}\,[N] = 1500\,[Kg] \cdot 9{,}81\,[\frac{m}{s^2}]$$

$$F_{Car} = 14715\ N$$

Force from the car divided between the four wheels

$$F_{Wheel} = \frac{14715\ N}{4} = 3679\ N \tag{9}$$

Used the rim's surface area for each model to find the pressure in pascals to apply on each model:

$$A_{Rim\ surface\ area}[m^2] = W_{Width\ of\ wheel}[m] \cdot \pi \cdot D_{Diameter\ of\ rim}[m] \tag{10}$$

Pressure (P_{rim}) applied to the rim's surface in negative Y-direction towards on the ground were found from this formula:

$$P_{Rim}\,[Pa] = \frac{F_{Wheel}\,[N]}{A_{Rim\ surface\ area}[m^2]}$$

By using these formulas, I got 11717 Pascals for the non-pneumatic and 14427 Pascals for the pneumatic tire.

3.1.5 Simulation of Preliminary Study

With the dimensions and the force specified the forces were applied on the models, like figure 13 shows.

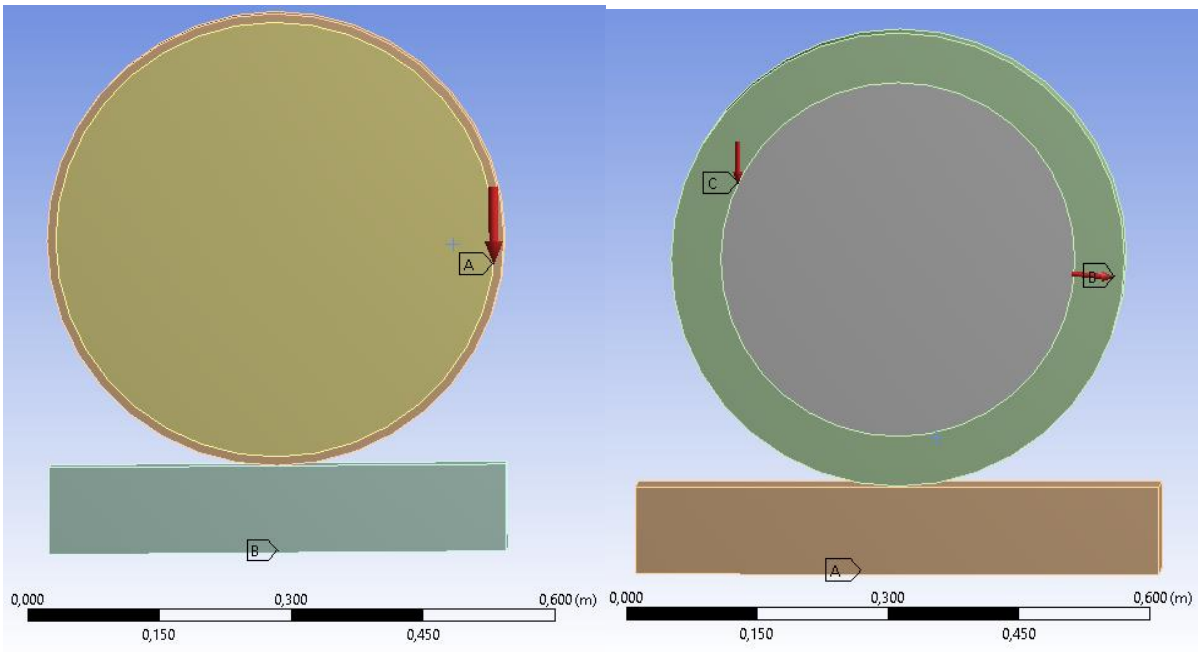

Figure 15: Forces and constrains on models from preliminary study

For both models, the concrete block was constrained at the bottom, to prevent it from moving under pressure. The pressure from the weight of the car, calculated for each model, were applied to the outer circumference area of each rim, acting downwards. These pressures are seen in as arrow A and C. Arrow B for the pneumatic wheel is the inflation pressure of the tire. All pressures are shown in Figure 15. The pressure acting on the inside of the tire wall that is in contact with the ground is seen as blue color in figure 16. This pressure was set to 280 kPa or 2,8 bars.

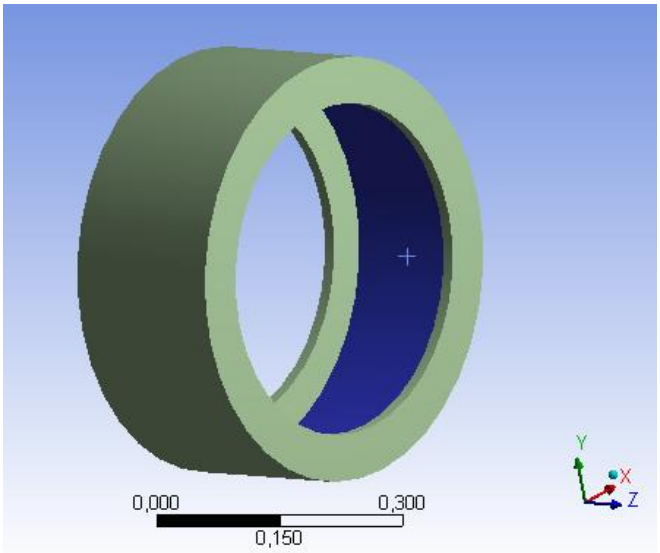

Figure 16: pressure inside pneumatic tire from preliminary study

3.1.6 Results from Preliminary Study

3.1.6.1 Frictional Contact Profile

First, we look at the frictional contact profile. On figure 17 we have the pneumatic tire and on figure 18 we have non- pneumatic tire. The first thing we notice is that both areas are dominated by sticking friction. The different friction types are described in chapter 1.2. Another noticeable difference is that the contact area for the non-pneumatic tire is larger than the area for the non-pneumatic tire. This is also positive in favor the non-pneumatic tire as a larger area of sticking friction is increasing the total grip limit.

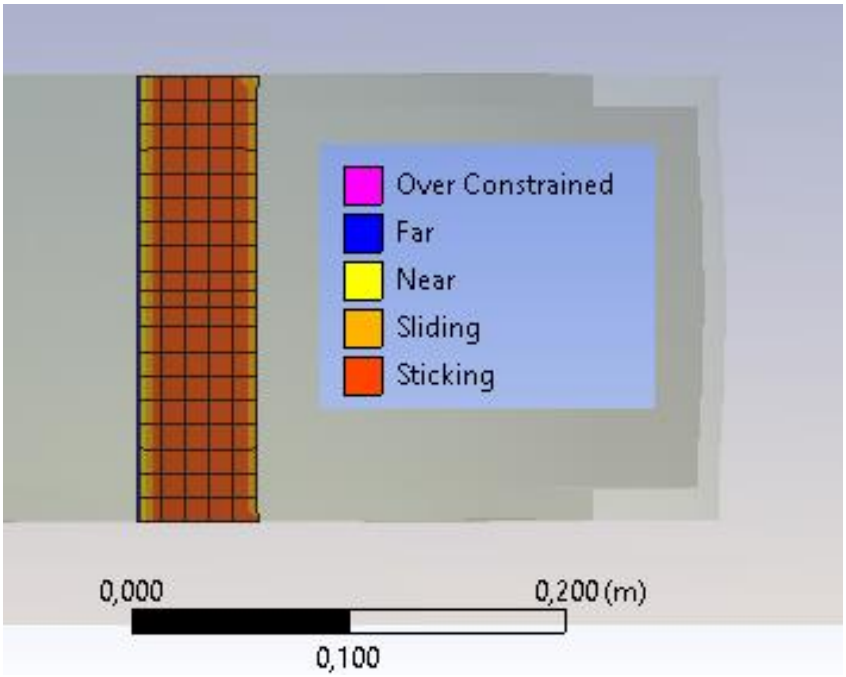

Figure 17: Frictional contact profile for pneumatic tire from preliminary study

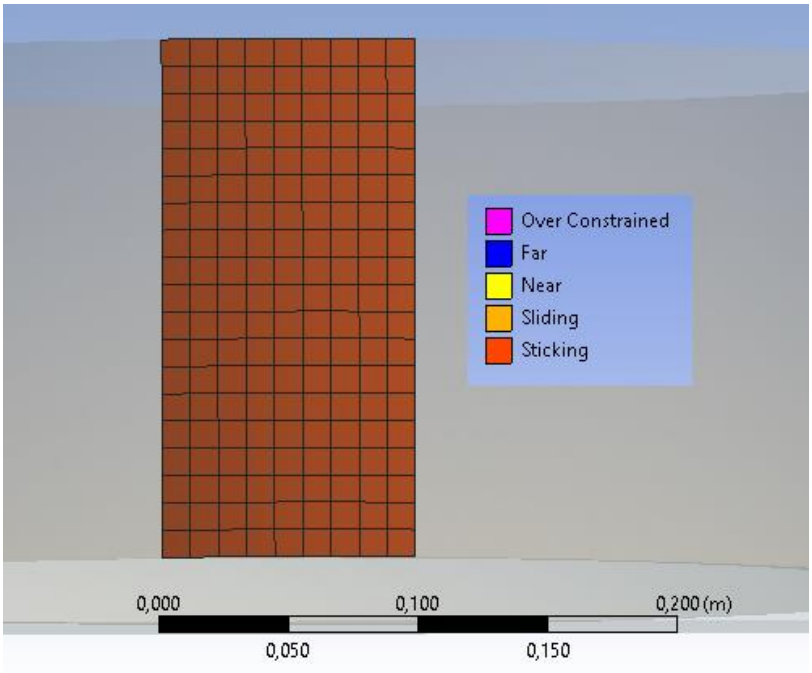

Figure 18: Frictional contact profile for non-pneumatic tire from preliminary study

3.1.6.2 Contact Pressure Profile

When comparing the contact pressure profile for the two models we can see that the pressure from the non-pneumatic model (figure 19), is more evenly distributed compared to the non-pneumatic model (figure 20). This is a result of the air distributing the force uniformly through the tire, where the non-pneumatic tire gets a more concentrated contact pressure in the center. When looking at the values however, we can see that figure 17's most represented pressure has values ranging between 10,5 kPa to 550 kPa, with some higher pressure peaks at the edges. The pressure profile for the non-pneumatic model shows a more concentrated pressure in the center of the contact area, with a peak large area with values ranging from 220 kPa to 237 kPa.

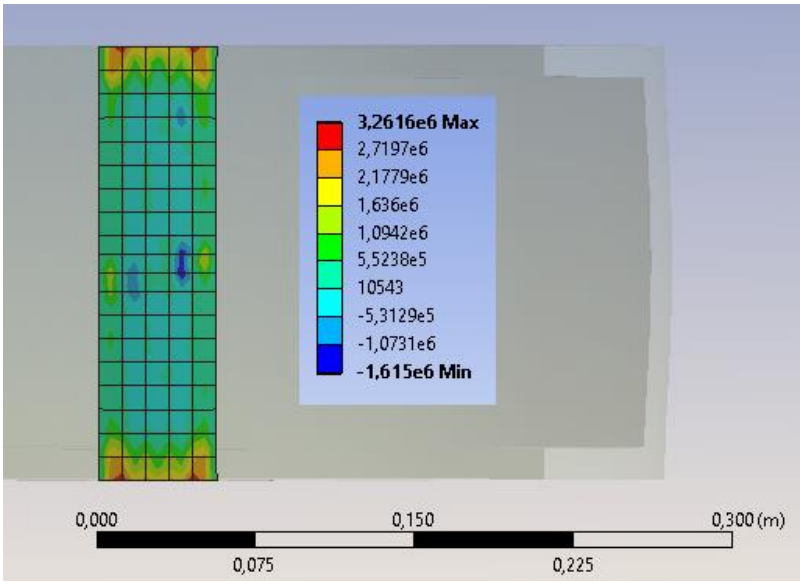

Figure 19: Contact pressure profile for pneumatic tire from preliminary study

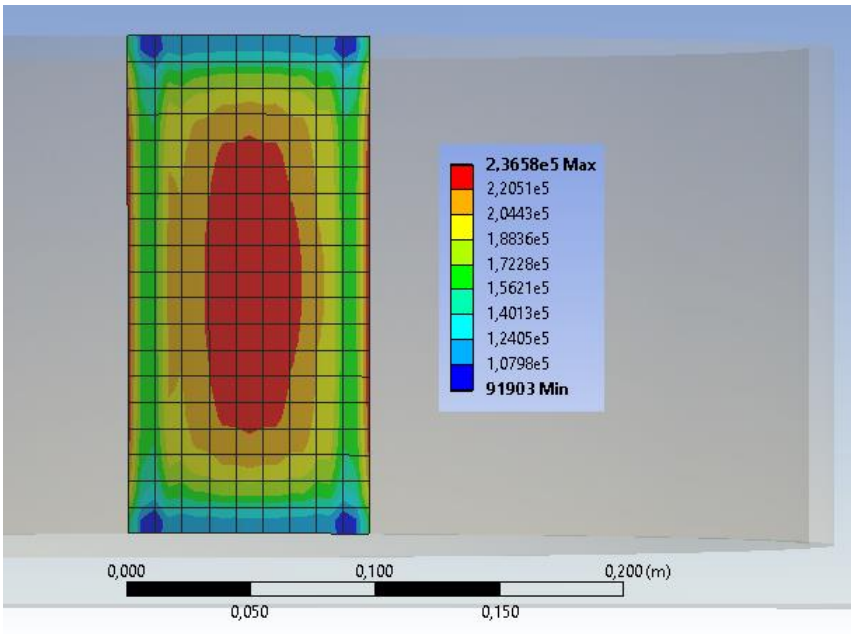

Figure 20: Contact pressure profile for non-pneumatic tire from preliminary study

3.1.7 Conclusion from Preliminary Study

In conclusion, the finite element approach to analyze the contact pressure profile on a car wheel works. We got 2 distinctive designs made comparable with the same boundary conditions and force inputs. The results show that there might be an increase in grip by changing the car wheel design to go from pneumatic tires to non-pneumatic tires. The contact pressure profile area was larger for the non-pneumatic tire as well as it had a defined large high-pressure concentration in the middle of the contact area. These are positive results and confirms that this is a topic that is worth looking more into.

3.2 MODELLING

After the preliminary study confirmed that this project is worth working on, more complex models were made. These were designed in inventor. The models were made as close to a real life model as possible. This is done by carefully designing a proper treading, dimensions and overall structure.

3.2.1 Treading

The process of designing the treading was to first look at pictures of winter tires with different patterns used today. I then proceeded to make drawings of how I thought a pattern could look like, before landing on the design in figure 21. The idea behind thread pattern is to make a high surface area while having grooves oriented in both longitudinal and lateral direction for water deflection and snow gripping. The pattern also makes for a preferred rotational direction to ensure that the water deflection happens properly.

To make the threading in Inventor I drew the right half of the blue highlighted sketch on figure 21. This pattern was then mirrored to make the left half of the tread but with a longitudinal (upwards on the picture) offset of 10,5 mm. With a now complete drawing covering the tire's width, I made an extrusion of 8 mm into the tire's surface to separate the tread blocks with grooves. This extrusion was then applied a circular pattern around the tire's circumference at a number high enough to make the pattern interfere with itself again, making up a tread pattern that is the same all around. When having a pleasing pattern, Inventor's fillet option was used to trim the edges of the tire making realistic tire shoulders. These were made by making an arched line with a radius of 8 mm. 8 mm, the same as the groove depth, were chosen to have a smooth transition between the tread and the sidewall.

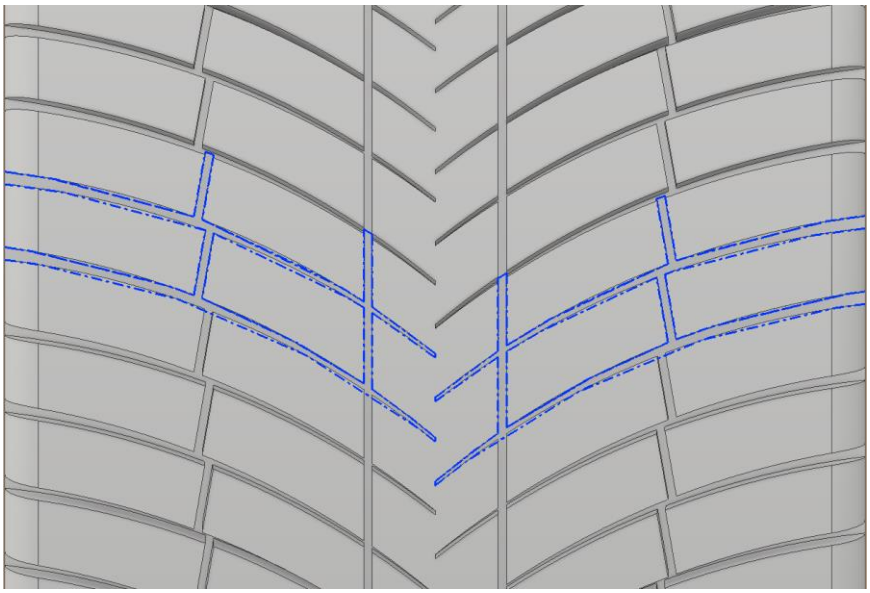

Figure 21: Tread design with initial sketch highlighted

3.2.2 Pneumatic Tire

The pneumatic tire model was made like a 205/55/R16 radial tire. Like chapter 2.3 tire anatomy explained, there are many components imbedded the rubber of the tire. I have included the ones that has an impact on the characteristic for a tire applied with vertical force. This leaves me with the sidewalls, steel belts, cap plies, carcass and treading. The finished tire model is shown in figure 22.

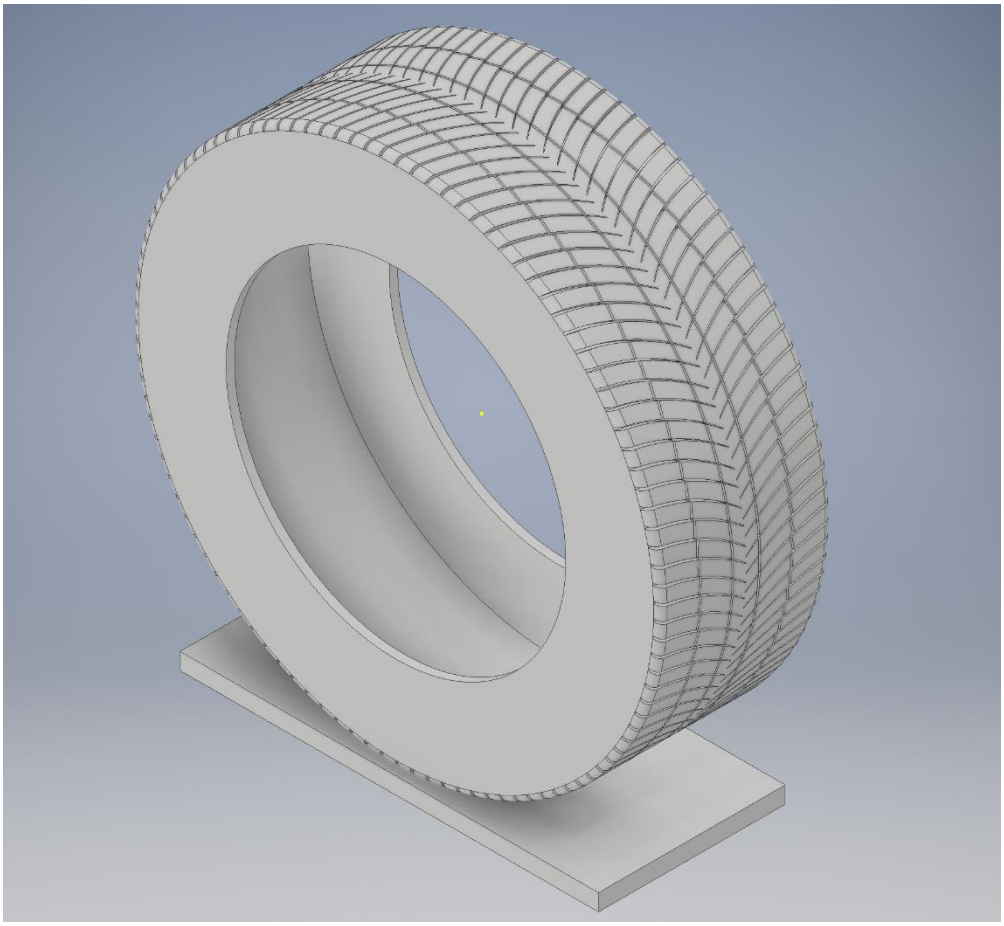

Figure 22: Pneumatic tire model from Inventor

3.2.2.1 Dimensions

The details of the dimensions used for the 205/55/R16 tire is presented in table5.

Part of tire	**Size [mm]**
Outer diameter of tire	632
Tire width	205
Groove depth winter tire	8
Total rubber thickness	15
Radius of rounded tire shoulder	8
Sidewall thickness	10
Sidewall height	105
Rim diameter	406

Table 5: Dimensions used for pneumatic tire sketch

3.2.3 Non-Pneumatic Tire

The non-pneumatic tire shares a lot of the same features as the pneumatic model. Other than designing it airless compared to air-filled, the size parameters were kept the same between the two wherever possible.

3.2.3.1 Design

The design for the non-pneumatic model was also made in inventor. I copied the treading from the pneumatic model and redesigned everything inside the rubber's inner circumference. This included the removal of the sidewalls, carcass, steel belt and cap plies from the pneumatic tire. Then I started by making the rim represented by a solid cylinder in the center. Between the rim and the rubber, curved plates are added to act as springs, these curves had an angle of 136 degrees and a thickness of 2 mm making a total number of 120 springs. The design is inspired by the Bridgestone's model of a pneumatic tire (seen on the right at figure 10). Even though this analysis doesn't look at a dynamic simulation with rotational movement, the design is made for a defined rolling direction. By looking at the model on figure 23, the preferred rolling direction according to both the orientation of the treading and the springs, is in clockwise direction. That way the treads can have optimal water deflection and we avoid unwanted shear stress on the springs.

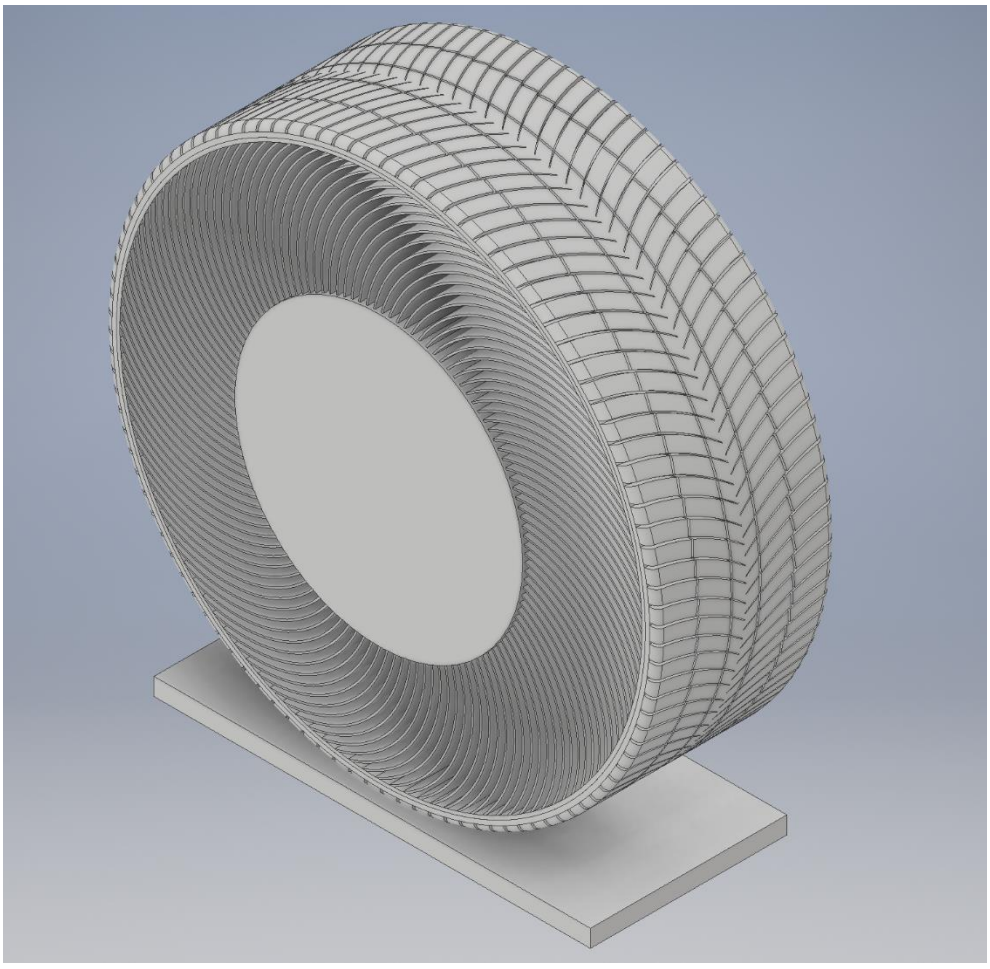

Figure 23: non-pneumatic model captured from Inventor

3.2.3.2 Dimensions

The dimensions of the non-pneumatic tire are placed in table 6.

Table 6: Dimensions used for non-pneumatic sketch

Part of tire	**Size [mm]**
Total Diameter	632
Tire width	205
Rim diameter	330
Ring thickness connecting springs and rubber	2
Height of spring area	134
Groove depth	8
Total rubber thickness	15

3.3 ANSYS WORKBENCH

After designing the models in Inventor, they were imported to ANSYS workbench 18.0, where physical inputs and simulations could be applied.

The idea with the simulations in ANSYS workbench are to have as similar boundaries to both simulations as possible, leaving the difference to be down to the implementation of springs and their characteristics. By doing this we mitigate the different parameters to have results that are purely determined by the difference of having air or not in the models. More details will follow in the sub-chapters below for each model. Instead of applying a force on the rim equal to the weight distributed from a car, a displacement was set to the ground plate. This was acting upwards onto the tire. The value of the displacement was corrected by looking at the reaction force on the ground. This reaction force was aimed to match a force equal to a car's weight.

3.3.1 ANSYS Workbench Static Structural Analysis Setup

The simulations in ANSYS Workbench were performed with their feature Static Structural Simulation, which uses finite element method when solving problems (see chapter 2.3). ANSYS uses the material properties, support conditions and loading conditions to solve equations for each node in all its degrees of freedom.

The procedure for setting up a static structural simulation is shown in figure 24. The first step is specifying the materials, and their physical properties. Then we create the geometric model, which can be drawn in ANSYS Workbench's own integrated sketching program DesignModeler. Or the geometry can be imported from other CAD files like Inventor, as done in this thesis. After the geometry is complete we proceed to defined mesh and apply forces and constraints before solving the model. The details of my inputs are presented later in this chapter.

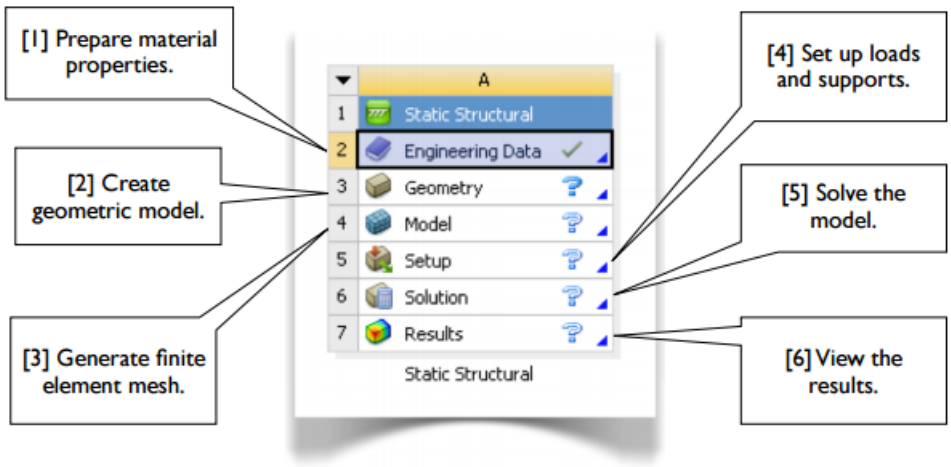

Figure 24: Static Structural Simulations [29]

3.3.2 Pneumatic Models Tried Before Ending Up with the Final Model

During the work on this thesis, many different models were tried before ending with one method of simulating the tire. This was especially true for the pneumatic model. In real life there are many non-linear materials used in a tire to give it the correct properties. As this thesis is limited to using linear materials, due to time restrictions and computational power, making them behave like a real tire was challenging. In a real tire there are several materials used to maintain the tire's shape in addition of being inflated (as listed in chapter 2.1.1). The same materials however is not responsible for handling the external stresses due to compression by the contact surface. This behavior, discovered during the thesis work, is not possible to simulate using linear materials.

The early models for the pneumatic tire included different materials imbedded into the rubber to represent the steel belts and carcass. They were both applied as a solid plate in the middle of the circumference of the rubber in one model, as well being introduced as hundreds of separate pins crossing the tire width in another model. Both models worked great to maintain the structure under inflation. However, these materials were also the ones taking up all the stresses applied from the ground. This gave the simulation behaviors not representable for a real life pneumatic tire but more like a solid cylinder.

After scrapping the idea of having many linear materials imbedded in the rubber, a model with two components was tried. This included two bodies; one for the ground, and one for the entire pneumatic wheel, combining the different material properties of a tire into one material. As this rubber had to be stiff enough to withstand the internal pressure, it also turned out too stiff to give a pressure profile resembling a pneumatic tire. This pressure profile had only 2 pressure points, one on each sidewall and zero pressure in the center. This model also had to be scrapped as it weren't considered accurate enough to be used.

After some trial and error with different models, the design and properties of the final pneumatic model are described further in the chapter. The model was made by having 3 bodies; the ground, the treading and the two sidewalls. By doing this the materials properties could be changed to represent the compound used for a real tire. As the tread had withstand higher stresses, this has a higher Young's modulus than the sidewall. By doing this we also avoid having the area underneath the sidewalls concentrating all the pressure.

3.3.3 Materials

The materials used were the same for both models to mitigate errors when comparing the results. As this is a linear elastic simulation, custom materials were made instead of using materials ANSYS Workbench's material data base. However, the general materials in ANSYS Workbench were used as a basis when creating the new materials. Values like young's modulus and Poisson's ratio were copied from the material data base. This was done to have realistic properties but to neglect parameters as heat transfer and non-linear properties. The different materials used, and their properties, are listed in table 7.

Table 7: Material used for modelling in ANSYS Workbench

Material	Volume applied to	Young's module [MPa]	Poisson ratio
Concrete	Ground	30 000	0,18
Hard rubber	Pneumatic tread	400	0,47
Soft rubber	Pneumatic sidewalls	10	0,47
Custom material	Springs for non-pneumatic model	2600	0,4

3.3.4 Pneumatic Model

The pneumatic model was imported to ANSYS Workbench with a total of 3 bodies. These included the ground, the tire tread and tire sidewalls. The reason for not including the rim is to reduce excessive parts and limiting the unnecessary increase in complexity of the simulation. The same reason was behind replacing the pressurized air by a manually applied pressure. This is possible as this study does not look at how the air is affected, but rather how air helps maintain the tire structure and distributes the pressure through the tire. This behavior was presented in chapter 2.6 and thus justifying the use of a uniform pressure inside the tire.

3.3.4.1 Boundary Condition & Body Contacts

The contact between the tread and the sidewall were set to "bonded contact", this meant that the bodies were fused together and not relying on any pressure or glue to stick together. This was done to ensure that there was no pressure leakage through the model under applied pressure and strain. The contact between the tread and the ground was set to frictional contact.

A fixed constrain was applied to the top of the sidewall to prevent the pneumatic tire from moving (marked in blue on figure 25). As the tire was fixed the external force had to come from the ground moving towards the tire. This was done to ensure that the tire would behave correctly. It is easier to have errors in the simulations by moving the larger body consisting of smaller bodies connected, compared to having it fixed and moving the simpler structure. In real life the tire is in contact with the rim at the sidewalls. The car is then pressing down on both the sidewalls and thru the pressurized air. However, the contact pressure would not be different by doing it the other way around and moving the ground towards the fixed tire. Hence, why this is done in this thesis.

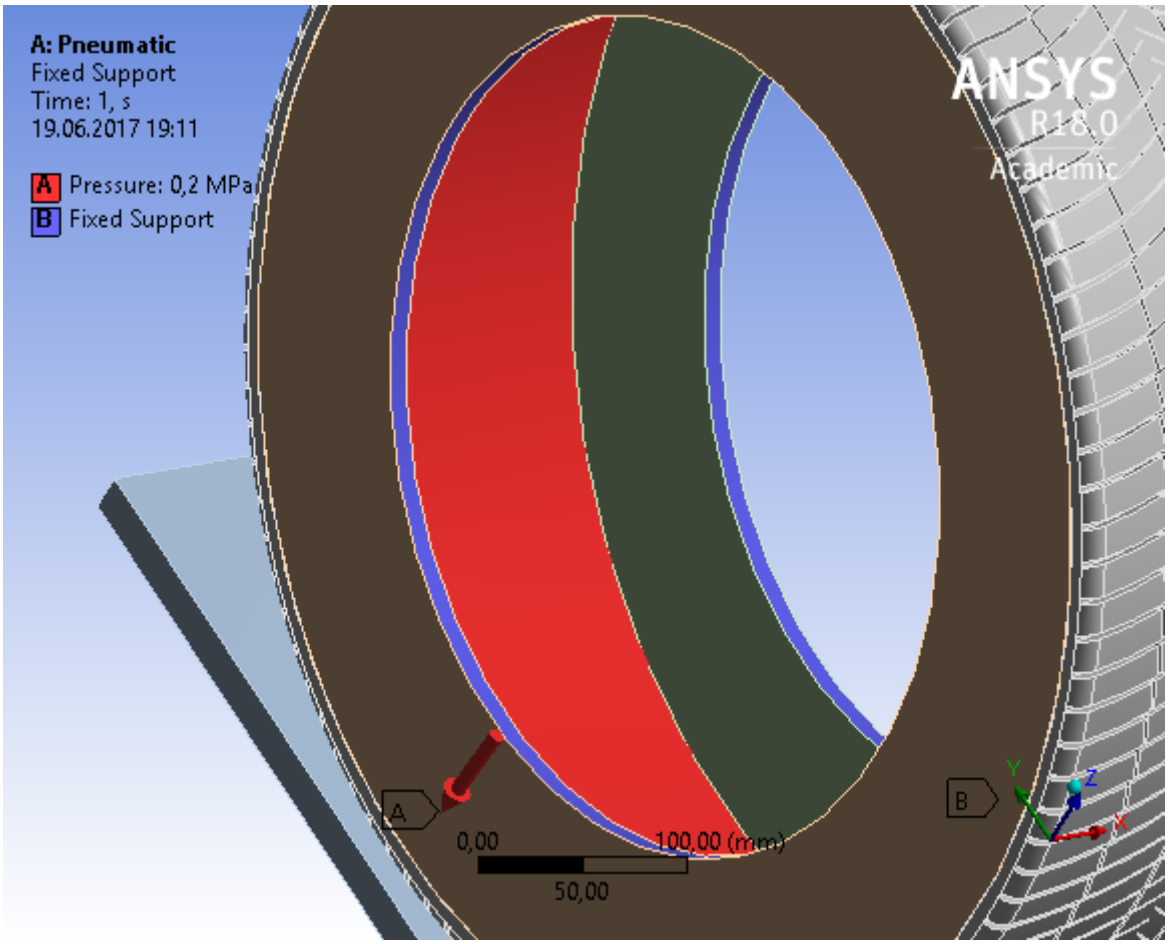

Figure 25: Fixed support and internal pressure applied to pneumatic model

3.3.4.2 Displacement and Force

For the tire to maintain its structure, a pneumatic pressure had to be applied. A pressure of 0,2 MPa, or 2 bars, was applied to the inner part of the rubber acting outwards (seen in red on figure 25). A 2 bar pressure is used as this is a pressure value representative for a 205/55R16 tire with a car weighing around 1200 kilograms. [30]

With both a fixed support and a force replacing air pressure, the ground plate was moved onto the tire, aiming for a reaction force equal to ¼ of a car's weight. The reaction force is calculated by ANSYS Workbench from the displaced body, the ground. This can in other words be seen as the force acting from the car, thru the wheel and to the ground.

At first the simulation was ran without moving the ground plate. By only applying the internal pressure the tire had a deformation on the center of 5 mm. As 5 mm deformation due to the internal pressure was reasonable, the ground displacement was added to achieve a reaction force close to 2979,3 N, equaling 300 kg (300 kg * 9,81 m/s^2 = 2943 N). With a displacement of 7 mm on the ground, the reaction force was 2979,6 N. A car with that reaction force on each wheel, considering a 50/50 weight distribution would weigh 1213,6 kg (2974,6 N /9,81 m/s^2 = 303,4 kg. and 303, kg * 4 = 1213,6 kg).

3.3.5 Non-Pneumatic Model

The non-pneumatic model was structurally more complex than the pneumatic model, because of the high increase in number of bodies due to the springs. There were a total of 120 springs in this model. Before importing the CAD model to ANSYS workbench, the bodies had to be defined to be able to specify the material later. The rim, springs, and a ring around the outer circumference of the springs, were combined into one body (see figure 26 for close-up of springs). This left the model with 3 bodies; the springs, rubber tread and the ground block.

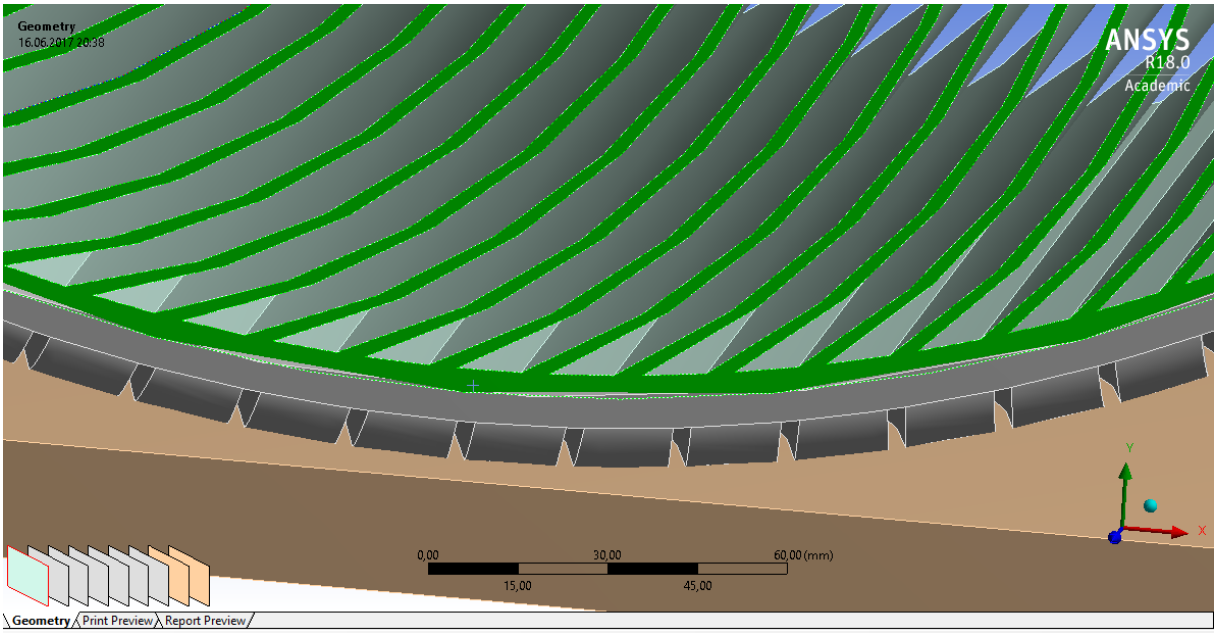

Figure 26: Close-up of the springs and connected ring merged to one body

3.3.5.1 Boundary Conditions & Body Contacts

Similar to the pneumatic model, the tire was constrained. The rim surface was applied a "fixed support", highlighted in blue on picture 27, to ensure correct behavior and zero movement under strain from the ground plate. The springs and the rubber were "bonded contacts" to prevent relative movement between the two. The last contact, between the tread and the ground was again set to "frictional contact".

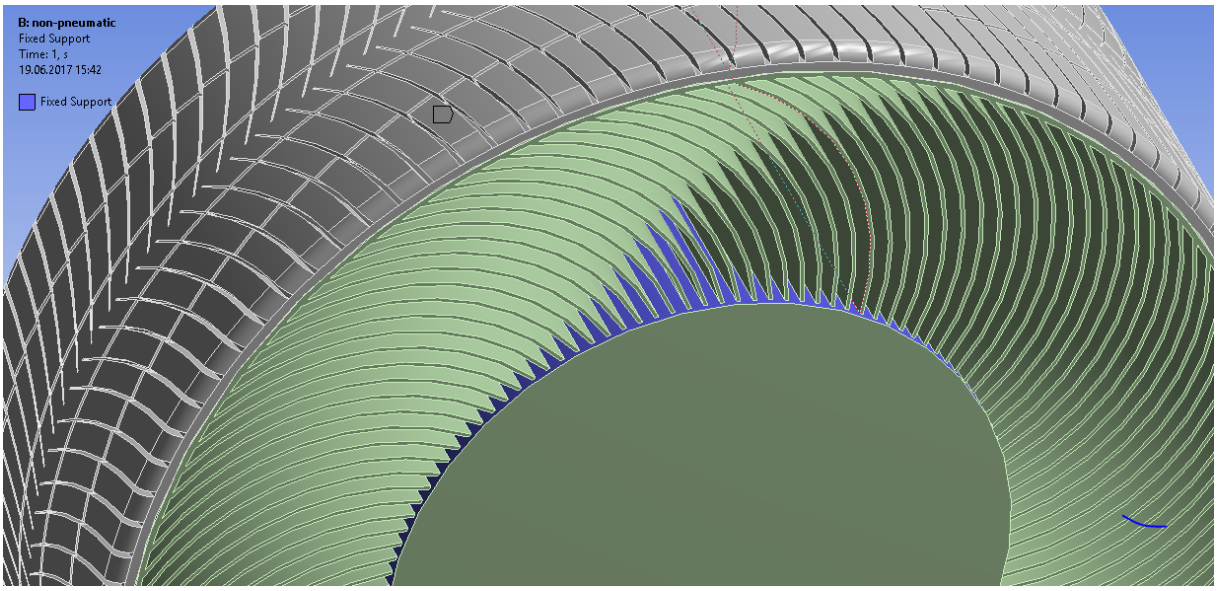

Figure 27: Fixed support, highlighted blue, added to the non-pneumatic model

3.3.5.2 Force and Displacement

The force in this model defined as a displacement of the ground. The level of displacement was set to match the total deformation of the pneumatic model. As the pneumatic model had deformation cause by both internal force and external displacement the total deformation was 7,9 mm. By having the displacement determined, the aim was to get a reaction force close to the pneumatic model of 2979,3 N. As all inputs were the same between the models, the Young's modulus (value of stiffness) for the springs were the only parameter separating the two models. After optimizing the Young's modulus, the reaction force ended up at 2976,6 Newtons. This was only 3,3 N off, which is a very satisfiable number. This divided by the gravity of 9,81 m/s^2 gives a weight of 303,7 kg. Multiplied by the 4 tires gives a car weight of 1214,8 kg. This is only a 0,01 % difference to the pneumatic model, making a common level force for both models when comparing the pressure profile in the results.

3.3.6 Meshing

To cut down the run time when adjusting the models, loads and boundary conditions were applied using a coarse mesh density. This made the models solve quicker and initial input errors could be solved in a shorter time. When the simulations solved and results were produced, the mesh density was increased to get more accurate results. A mesh sensitivity analysis was also performed to see the effects of mesh density on the results.

3.3.6.1 Mesh Sensitivity Analysis

The mesh sensitivity analysis was performed on the non-pneumatic model. Two size parameters were changed when performing this analysis; the relevance center and the span angle center, at the levels; coarse, medium and fine. The mesh element type was set to automatic, mainly generating tetrahedral elements. The concrete block was the only object

consisting of quadrilaterals. The meshing, parameters and values are displayed in table 8, while the graphs made from these numbers are presented in figure 28.

Table 8: Mesh sensitivity analysis data

Relevance center	Span angle center	No. of elements	No. of nodes	Reaction force [N]	Equivalent stress max [MPa]	strain energy [MJ]	Structural error [MJ]
coarse	**coarse**	150965	283583	37467	61,958	406,62	2527,4
coarse	**medium**	153442	287630	39338	78,934	399,4	3521,2
coarse	**fine**	170127	322336	42194	70,944	462,79	2080,9
medium	**coarse**	258265	492013	8123,9	40,932	27,25	122,14
medium	**medium**	259785	494600	8082,8	42,096	23,695	123,15
medium	**fine**	281469	539466	7743,6	43,021	23,765	123,19
fine	**coarse**	471965	905469	3577,1	32,586	2,3353	5,8724
fine	**medium**	475401	911326	3537,6	31,974	2,3872	5,2925
fine	**fine**	510859	979439	3438,8	32,935	2,3335	5,8221

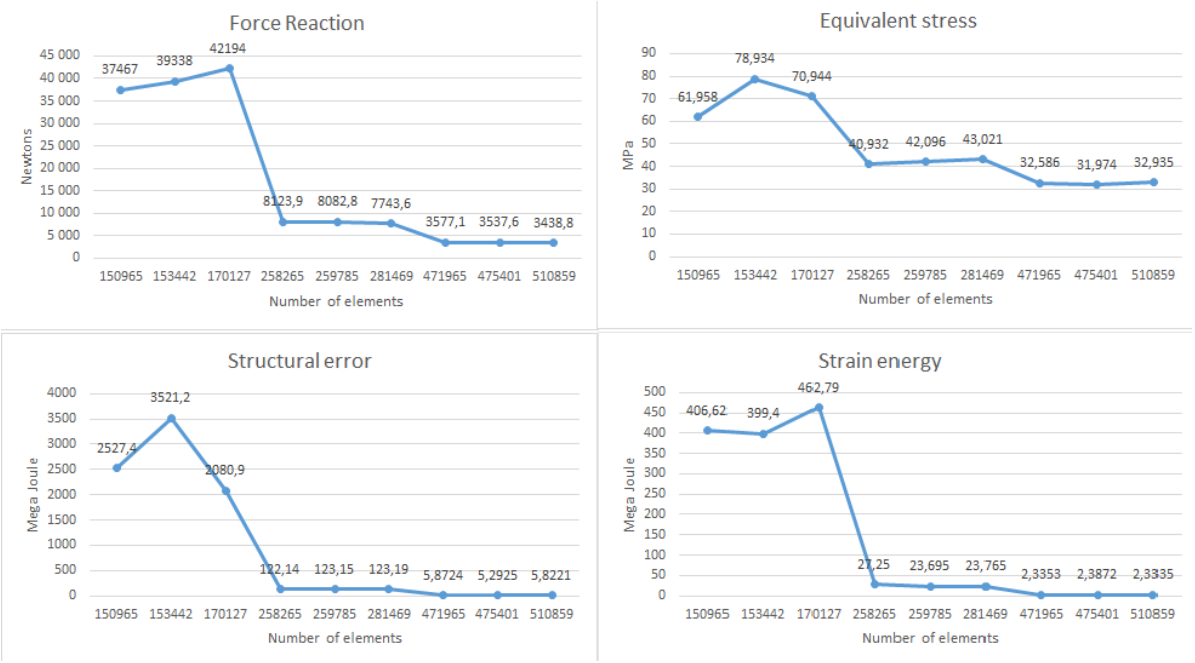

Figure 28: Mesh sensitivity analysis graphs

This analysis shows a major difference in result values over the different mesh densities. The relevance center is the biggest factor, compared to the span angle center, as it determines the sizing of the elements. When increasing the relevance center one level (e.g. coarse to medium), the number of elements and nodes almost doubles, while increasing the span angle center gives an increase in element number of around 10%. It's clear that the three results with the coarse meshes fluctuates at high levels, while medium and fine mesh converge better. A finer mesh was also tried by manually decreasing the size limit for the smallest elements. However, by doing this the simulation weren't able to solve. With the information provided by this analysis, the conclusion is that the usage of the finest mesh density for both relevance

center and span angle center gives the most trustworthy results. Hence, why these mesh settings are applied when solving the simulations in ANSYS Workbench.

3.3.7 Mesh of the Pneumatic Model

As mentioned earlier both the relevance center and span angle center were set to fine. As the FEA in this thesis focuses on the contact area, a refinement was added to the tire treading at the contact area. This allows for a higher mesh at user defined areas. The refinement was set to 1, which means that each element is divided one time over both the x and y axis. By doing this we have increased the number of elements by four times at the defined area. This allows for higher resolution on the results and the graphical presentation of the results. The total number of elements were increased to 661742. A picture of the mesh with refinement is shown in figure 29. Although this mesh density was considered appropriate, a refinement of 2 was also tried. This divided each element two times in every direction providing 4*4=16 elements for every element chosen. This brought the total number of elements to 1,4 million which brought a too high complexity for the computer to solve.

3.3.8 Meshing of the Non-Pneumatic Model

This model was meshed with the same procedure as for the pneumatic model. Both mesh density settings were set to fine. When the wanted reaction force was achieved the "mesh refinement" was added in the same manner as for the pneumatic model. This gave a total of 952613 elements. Figure 29 shows how the tread was meshed, as the tread had the same mesh for both models. The structure of the elements was still set auto which gave tetrahedral elements on the tire and quadrilaterals for the ground block.

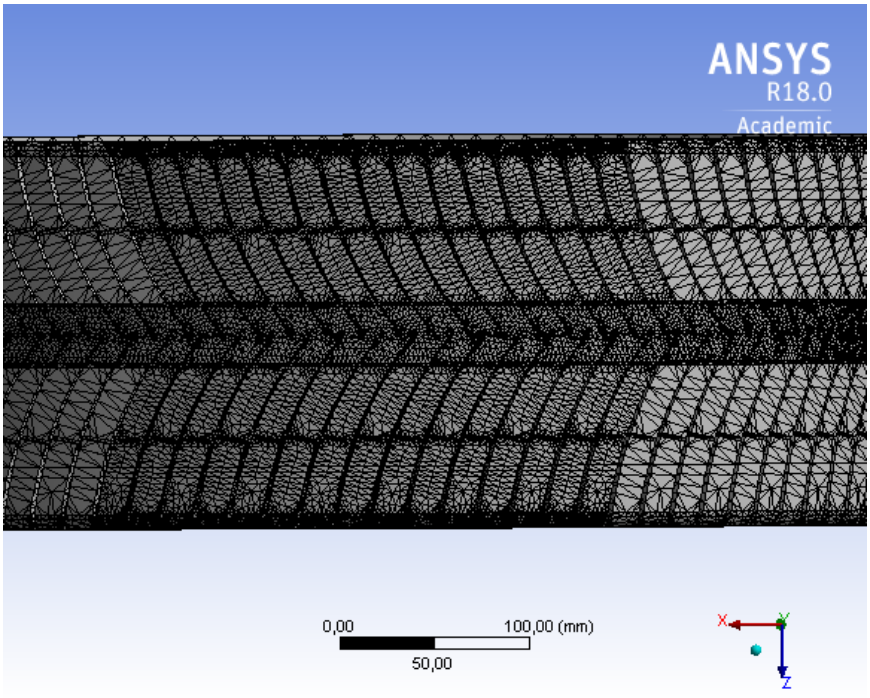

Figure 29: Meshing of the tread on pneumatic and non-pneumatic model

4 RESULTS & DISCUSSION

The results, comments and discussion of the results are presented in this chapter, both discussing the positive and negative sides of them.

4.1 PNEUMATIC MODEL

When looking at the results for the pneumatic model, we can conclude it to be a good model. The geometry and visual of the model looks great, both in respect to detail and sizing. By looking at it, there is never any doubt if it's a car tire, especially with the presence of the detailed treading.

4.1.1 Deformation

With the inputs described in the methodology the deformation was as shown in figure 30. The deformation is affected by two external factors; the pressure applied from the inside simulating air pressure, and the strain from the plate pushing in on the tire's outside. The rubber characteristics are working properly on keeping the tire structure from bulging outwards and becoming circular. The Young's modulus is not set too high either as it allows for some deformations due to the internal pressure alone. A real tire will also suffer from some expansion in the middle of the width under inflation, and that it what we are seeing on figure 30 as well.

The total deformation under the additional stress from the ground plate's displacement looks realistic. The highest deformations happen close to the contact area and with a maximum deformation of 7,9 mm located a about 20 cm to both sides of the contact, shown in red on figure 30. Figure 30 also shows how smoothly the transitions between the colors are with no sharp edges. This indicates that the solution has converged fully and has a satisfying mesh density. Although not having any experimental data to compare with, a maximum total deformation of 7,9 mm doesn't seem too far off from realistic values. This is 1,25 % of the tire's diameter. The total deformation of a real tire would also be dependent on the inflation pressure. However, as the ground plate is displaced at a constant 7 mm, the internal pressure wouldn't have the same impact on deformation as if the tire was applied a weight. Then a high pressure tire would keep its shape better than a low pressure tire, that would experience a higher contact area and deformation. The pneumatic model in this thesis has a realistic combination of deformation caused by both internal and external pressure forces.

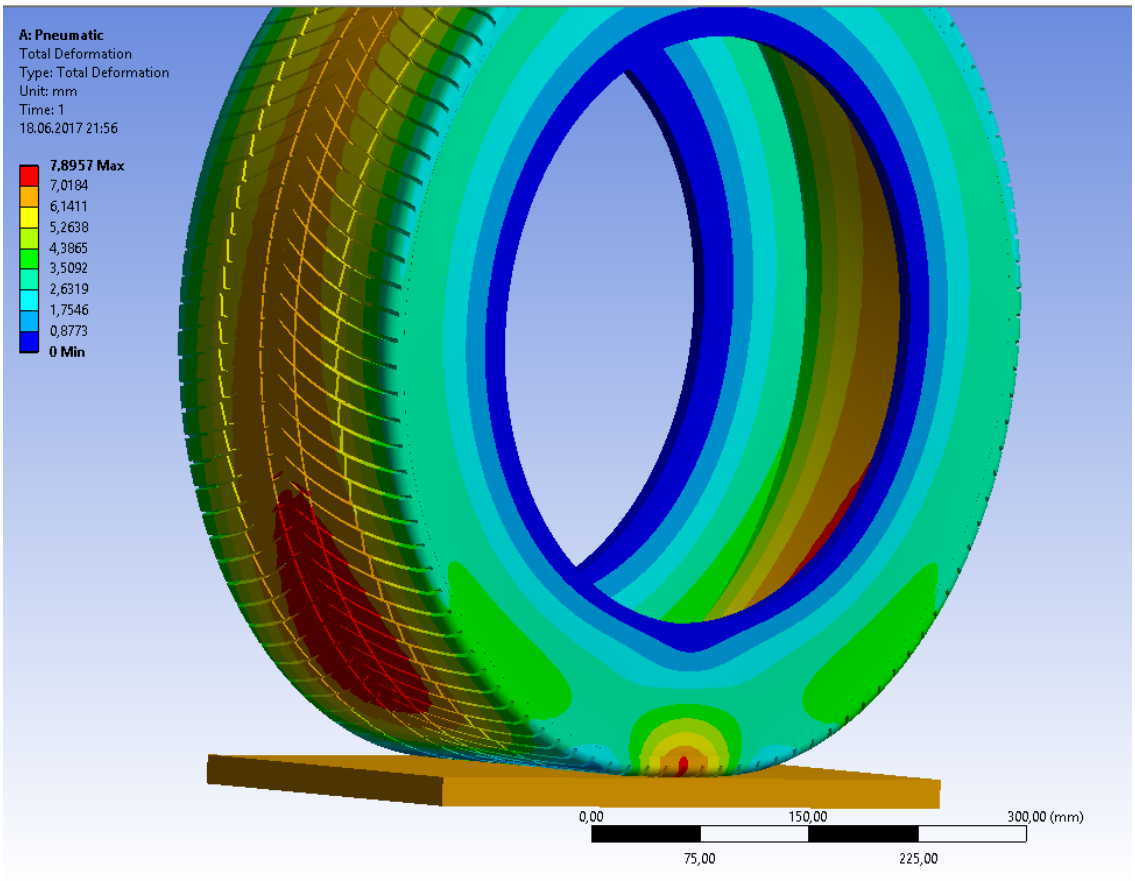

Figure 30: Deformation of pneumatic model

4.1.2 Pressure Profile

The pressure profile is given in figure 31. First of all, the smoothness of the figure indicates that the mesh was done correctly and that the results did converge. We can see how the pressure is distributed through the contact area between the tire and the ground. This is experiencing low pressure values at the blue area increasing towards the red. The average pressure over the middle area is not very high at pressures below 1,2 MPa. There are two areas that experience a pressure above 2 MPa, and that is on both sides of the tire, just below where the sidewall ends.

Having pressure concentrations on the edges under the sidewalls can be justified if we assume the tire to have a too low internal pressure (low tire pressure illustrated on figure 8). Isolated, a low tire pressure can give better traction on loose surface such as snow and gravel due to the increase in contact area and the tire's ability to deform over the surface unevenness. However, it is not recommended having a too low pressure for everyday driving as the wear on edges increases and heat generations happens quicker with a low tire pressure, leading to a risk of the tire cracking [31].

On the negative side questions can be raised on whether it would have been better to run the simulations using non-linear materials with different properties. As a real tire consists of around 10 components with different objectives, it is close to impossible to match the characteristics of all these components in one single material. Add that some of the components are non-linear and this simulation were performed with linear materials, due to time limitations and computational complexity of non-linear simulations. If time wasn't a factor a model of non-linear material properties could be preferable. The carcass should for example be able to be internally inflated to reach a certain volume, but not beyond this point. At the same time, the carcass should also have the characteristics of not being able to resist external forces. Only by having a non-linear material those characteristics can be achieved, and a very accurate model of a pneumatic tire could be made. Having said that, I believe that this model with a softer sidewall than tread, was the best way to present the pressures profile between the tire and the ground using linear elastic materials.

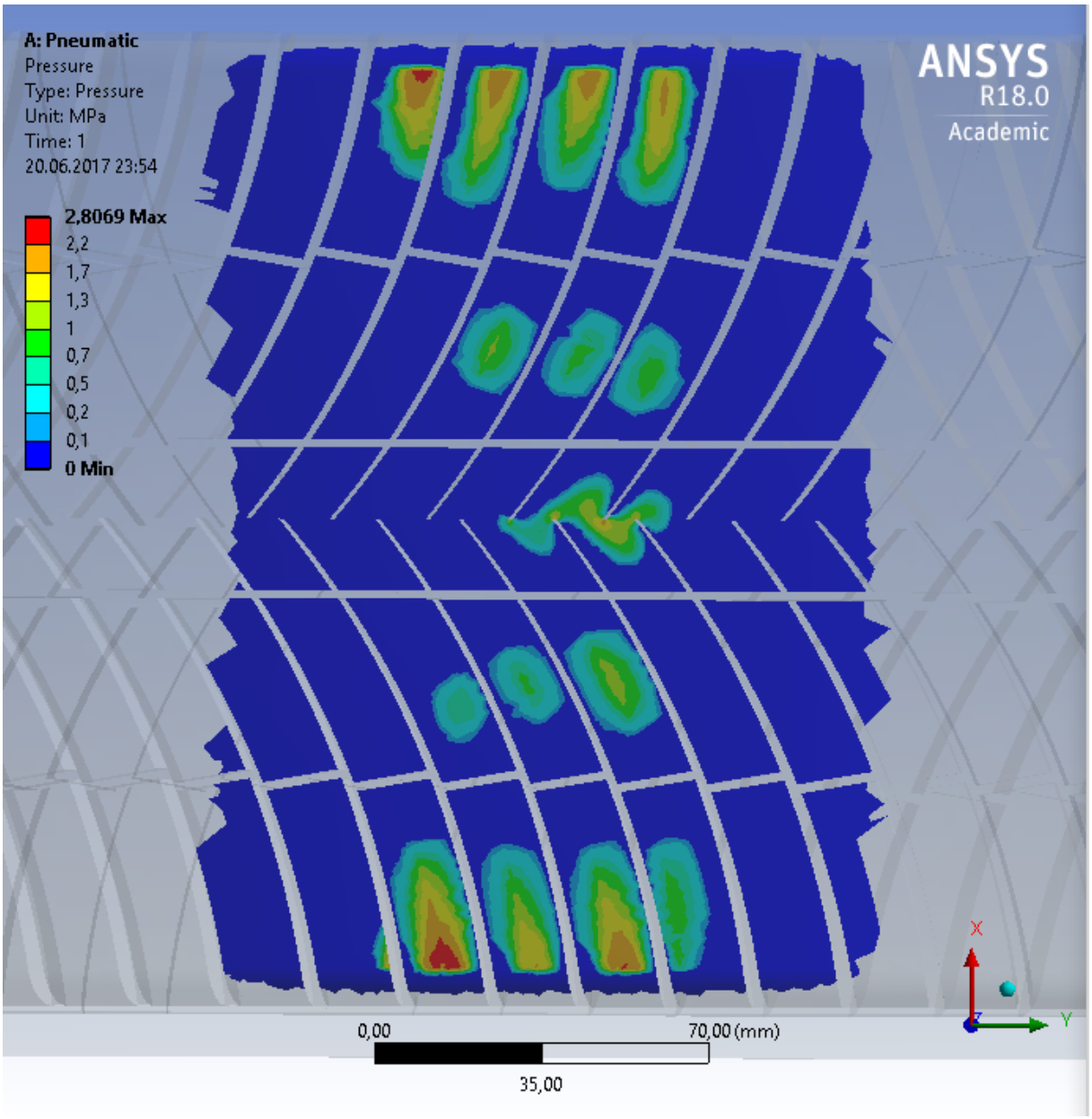

Figure 31: Pressure profile for pneumatic model

4.1.3 Equivalent Stress (Von-Mises stress)

The equivalent stresses are displayed on figure 32 and 33. Stress labels are also placed on the picture to make it easier to locate the different stress areas. We can see from the coloring that some of the high stresses are located inside the tire over the contact area, with a maximum value of 12 MPa. The other areas experiencing high pressures is in the grooves of the treading slightly offset to the contact area. This is the area where the max stress of 31 MPa occurs. Another thing to notice is that the stresses are generally higher in the center of the width than on the tire shoulders.

The stresses on the pneumatic model are a result of the internal and external forces. The distribution of the stresses makes sense as they are located where the highest deformation happens. If the model is run without including the ground plate, the stress would be distributed even at given width over the tire's circumference because of the pneumatic pressure. When compressed by the plate, the tread as one body, will have the highest stresses at its narrowest points. This is the reason behind the highest stresses being located in the bottom of the grooves.

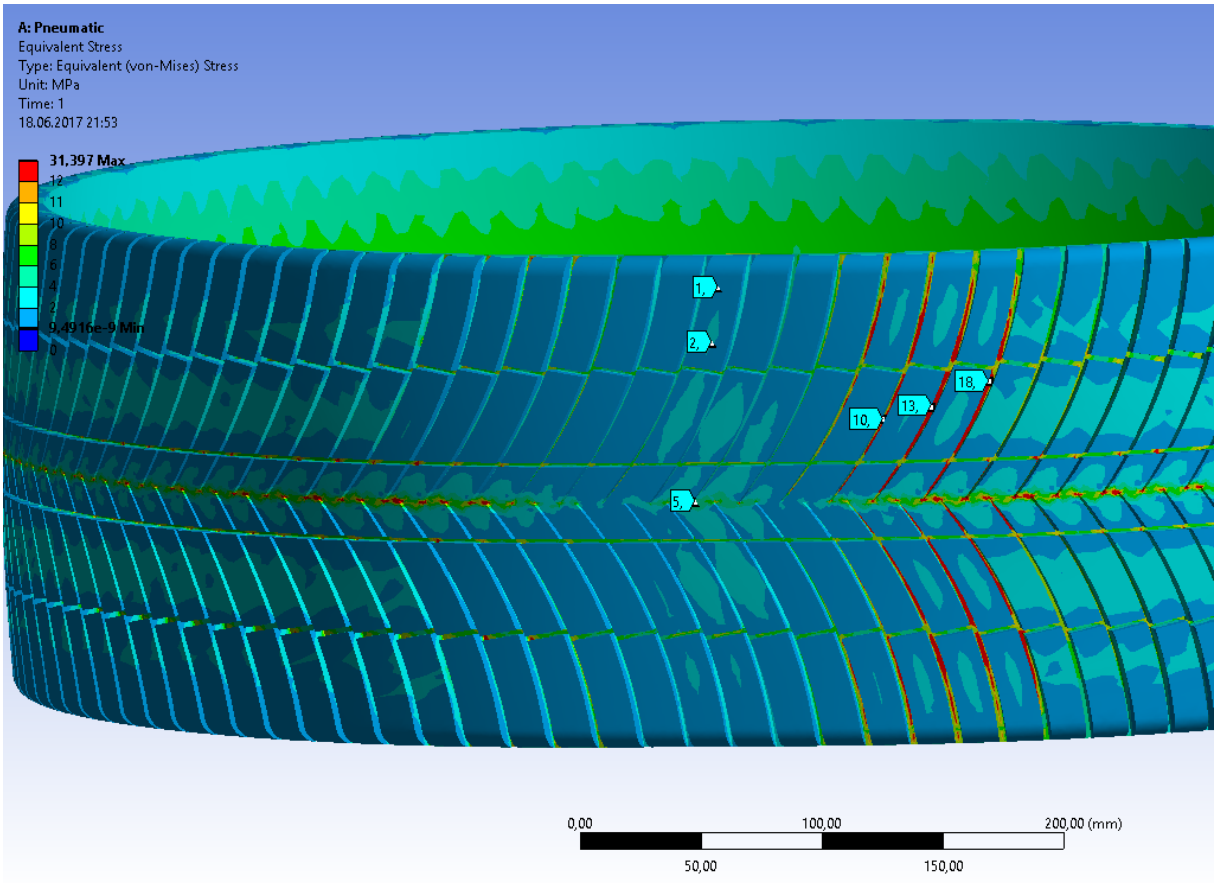

Figure 32: Equivalent stress on the outside of the pneumatic tire

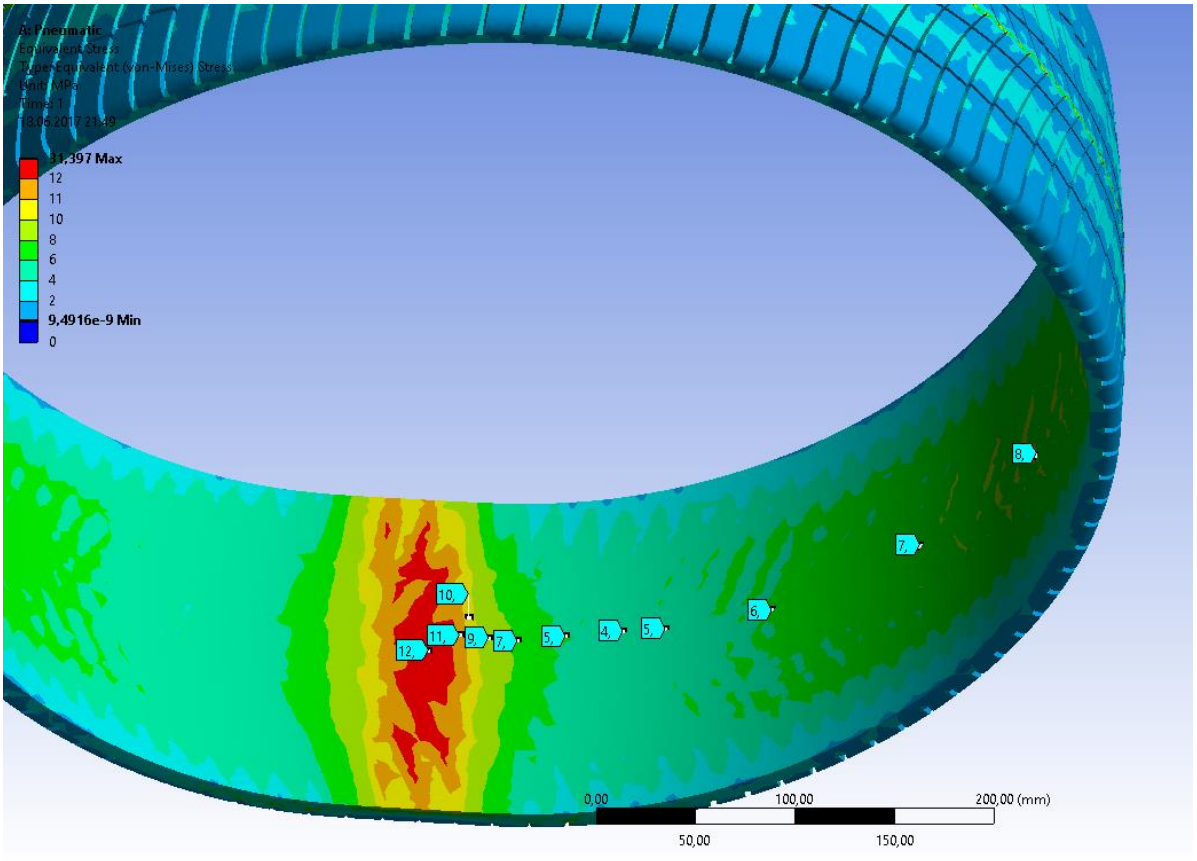

Figure 33: Equivalent stress on the inside of the pneumatic model

4.2 NON-PNEUMATIC MODEL

4.2.1 Deformation

The deformation for the non-pneumatic model is shown in figure 34. As the displacement of the plate was set to 7,9 mm. to match the total deformation of the non-pneumatic model, the deformation on the contact area is 7,9 mm. The highest deformation happens at the springs that are connected over the contact area. Even with a deformation of 8,7 mm, the springs still has good clearance between them.

The deformations of the model were as expected when the design was made. The springs behaved predictable just as visualized when sketching the model. The largest deformation happened in the middle of the spring that was connected to the rubber above the contact area. This deformation was a bit larger than the displacement of the ground plate. The length of the spring looks to be good as the compression of the spring never changes the angle of the attachment to the rim or tread. If this angle would exceed 90 degrees the structure might become unstable as the spring would be forced bent the opposite direction of what the ware designed to. This deformation indicates that this is a well-designed pneumatic tire model.

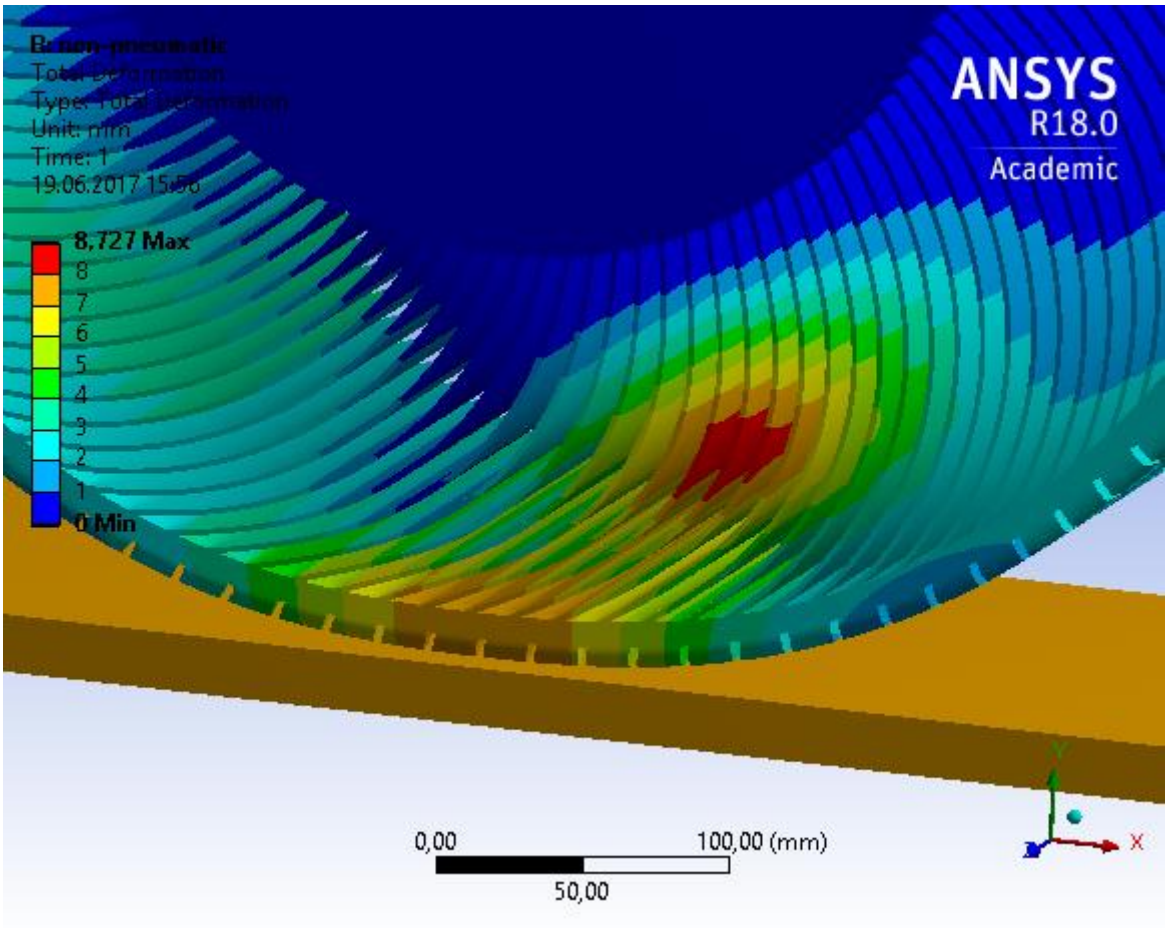

Figure 34: Deformation of non-pneumatic model

4.2.2 Pressure Profile

Figure 35 shows the pressure profile for the non-pneumatic model. Again, the figure is smooth and has no abnormalities in the pressure distribution. This shows that the meshing used were of a sufficient density. The pressure is for the most part uniformly distributed over the width of the tire over the contact area. The pressures are above 1,6 MPa on every tread block over that width. which is a good result in terms of pressure concentration thru the center of the contact area. That is a good representation of how the pressure profile should look like when comparing it with the theory presented in chapter 2.6.1. The maximum pressure of 4,4422 MPa occurs in the center of the profile. Both the value and location of the pressure is positive as the aim of this thesis was to see a pressure concentration in the pressure profile.

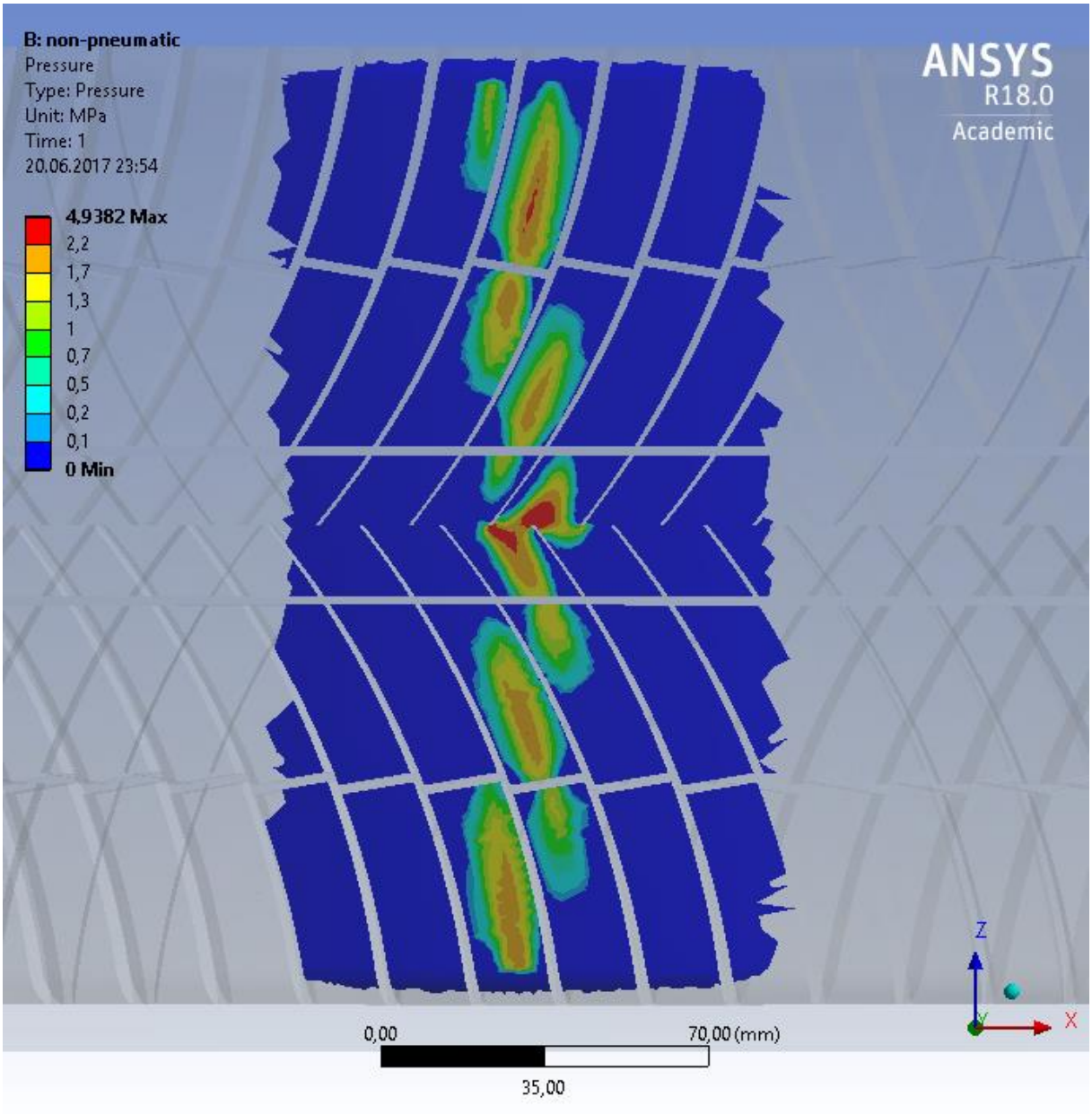

Figure 35: Pressure profile for non-pneumatic model

4.2.3 Equivalent Stress

The equivalent stress is displayed in figure 36. The labels are placed on key areas to highlight the stresses. We can see that the stresses are higher at the points where the springs are attached to the rim and the rubber compared to on the center of the individual spring. The maximum stress appears inside the rubber in the center of the contact area. This pressure was not visible on the surface of the treading but was located from the ANSYS Workbench function “Locate max stress”. This is the same point that had both the maximum deformation and maximum pressure. Having all of these at the same location over the contact area, can be seen as an indication that this is a good non-pneumatic model with predictable results.

Finding the stresses is not the main objective of this thesis, but it is still interesting to look at and can also be used to locate errors in the simulation, if there are any. These pressure values are also quite low and that makes looking for a material easier as the yield strength doesn’t need to be that high. There might be possible to use plastics as material for the springs. That being said, these values shouldn’t be used as design stresses before a simulation with non-linear materials have been tested against the results in this thesis.

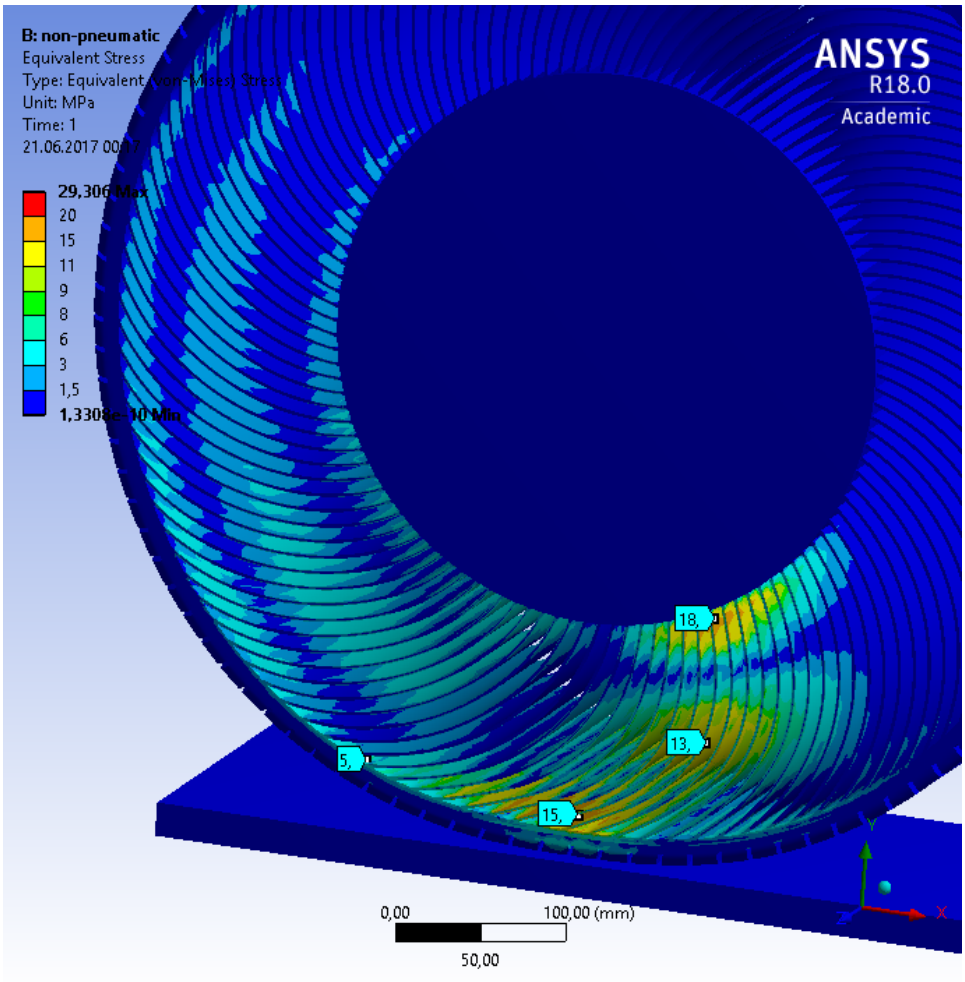

Figure 36: Equivalent stress for non-pneumatic model with stress labels highlighting interesting areas

4.3 Comparison of Pressure Profiles

Pressure profiles side by side with same pressure values on the color bar:

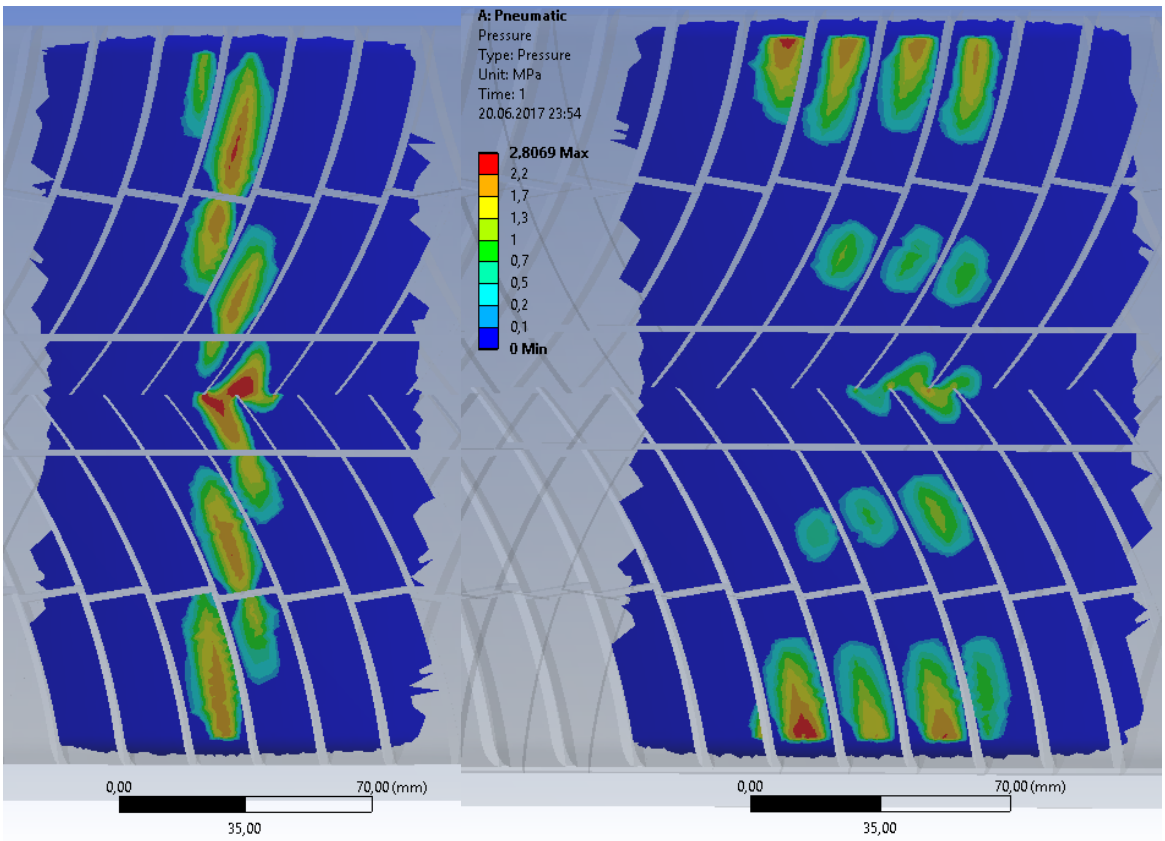

Figure 37: Side by side comparison of the pressure profiles. Non-pneumatic on the left and pneumatic on the right. Both sharing the same color bar pressure values

When comparing the two pressure profiles side by side we can more easily see the differences between them. Worth mentioning here is that the non-pneumatic model on the left is without its color bar. This is done to be able to have larger picture for side by side comparison, and the fact that the models share the same pressure values for each color makes this possible. The only difference being the maximum pressure that is not shown for the non-pneumatic model, but can be seen on figure 35 to be 4,94 MPa.

In the pressure profile of the preliminary report (see conclusion on chapter 3.1.7) we could see that a non-pneumatic model had a different pressure profile than a pneumatic model. This conclusion is complemented by the comparison of the two models in this thesis. The first visual difference is that the contact area of the pneumatic model is the largest of the two. The difference being the that the pneumatic profile is having 8 blocks in contact with the road compared to the non-pneumatic model's 6 blocks, when counting in longitudinal direction (left to right). This is also the truth despite that the ground block for the pneumatic model was moved 7 mm, which is 0,9 mm less than the 7,9 on the non-pneumatic model.

If we look at the pressure values across the mid-section of the tires, there is a clear trend. The pressures of the non-pneumatic model on the left is much more concentrated towards the center and has higher pressure values. The pressure concentrations of the pneumatic model

cover the longitudinal length to a larger extent than the non-pneumatic model, with approximately 4 tread blocks compared to approximately 2. This is positive results as the aim of the thesis is to prove that the non-pneumatic tire has a more concentrated pressure profile with higher pressure values.

5 CONCLUSIONS & FUTURE WORKS

5.1 CONCLUSIONS

After completing this study, we can draw following conclusions:

- The pressure profile does change when changing from a pneumatic tire to a non-pneumatic tire. The pressure profile of the non-pneumatic model showed that a more concentrated pressure over the center of the contact area. The pressure was both more evenly distributed over the tire width with higher average and maximum pressure values. This concentration of pressure is believed to increase the grip of a tire as the friction coefficient is a function of pressure.

- Finite Element Analysis looks to be a valid approach to analyze the pressure profile between two static objects.

- The increase in grip of a non-pneumatic tire is just one of the benefits. Other benefits are.
    - Less wear on the roads due to less need of studded tires. This decreases the maintenance cost for the roads.
    - Consumer benefit of not risking a puncture and flat tire.
    - Depending on the material used for the springs, the tire characteristics won't be as affected by temperature fluctuations as the pressure inside a pneumatic tire.

- The study is performed with linear materials only. This should be considered when looking at equivalent stresses and the pressure values of the models. Especially the pneumatic model as its materials has a more non-linear behavior.

- Though further studies are required, the non-pneumatic tire has the potential to become the next revolutionary milestone in the history of winter tires.

5.2 FURTHER WORK

- A Finite Element Analysis could be performed with the use of non-linear materials to ensure that the behavior of, especially, the pneumatic model is correct.

- Compare the results with lab testing of both a conventional tire and if possible one of the other manufacturers non-pneumatic concepts.

- Aim to build a prototype of a non-pneumatic wheel designed especially for the arctic conditions.

6 REFERENCES

[1] Noikan Tyres, "Noikan Tyres," 2016. [Online]. Available: https://www.nokiantyres.com/company/about-us/history/. [Accessed 2 December 2016].

[2] BPEARSON, "Cenco Physics," 2010. [Online]. Available: http://blog.cencophysics.com/2010/02/coefficient-of-friction/. [Accessed 15 December 2016].

[3] The engineering toolbox, "The engineering toolbox," [Online]. Available: http://www.engineeringtoolbox.com/friction-coefficients-d_778.html. [Accessed 10 December 2016].

[4] Statens Vegvesen, "Vegvesen.no," 2015. [Online]. Available: http://www.vegvesen.no/_attachment/1159148/binary/1086284?fast_title=Drepte+i+vegtrafikken+-+%C3%85rsrapport+2015.pdf. [Accessed 20 November 2016].

[5] P. B. B. B. A.-C. O. a. B. F. Hanne Krage Carlsen, "PMC - US national library of medicine, national institute of health," 2016. [Online]. Available: https://www.ncbi.nlm.nih.gov/pmc/articles/PMC4924078/. [Accessed 1 Desember 2016].

[6] Statens vegvesen, "Flere pigger gir mer svevestøv," 4 April 2015. [Online]. Available: https://www.vegvesen.no/fag/fokusomrader/Miljo+og+omgivelser/Forurensning/Luft/nyheter/Flere+pigger+gir+mer+svevest%C3%B8v. [Accessed 4 March 2017].

[7] M. K. a. L. S. P. Norris Shippen, "REVIEW OF STUDDED TIRES IN OREGON," Oregon Department of Transportation, Oregon, 2014.

[8] D. Kopeliovich, "SubsTech," 2016. [Online]. Available: http://www.substech.com/dokuwiki/doku.php?id=mechanisms_of_wear . [Accessed 7 April 2017].

[9] BayTires, "Baytires," [Online]. Available: https://www.baytires.com/faq. [Accessed 3 Mai 2017].

[10] Apollo, "Apollotyres," [Online]. Available: http://traditional.apollotyres.com/en-eu/making-of-a-tyre. [Accessed 26 Mach 2017].

[11] *Winter Tyres v Summer Tyres: the Truth!*. [Film]. England: Auto Express, 2011.

[12] imgur, "imgur," 11 March 2014. [Online]. Available: http://imgur.com/gallery/xlI22. [Accessed 25 May 2017].

[13] D. Evans, "Which?," 2011. [Online]. Available: https://conversation.which.co.uk/motoring/winter-tyres-snow-weather-cars-buy/. [Accessed 22 May 2017].

[14] J. Fenske, "Winter tyres explained," Youtube.com, 2014. [Online]. Available: https://www.youtube.com/watch?v=8OifbH5siF0. [Accessed 5 May 2016].

[15] P. Cheney, "The globe and mail," 2016. [Online]. Available: https://www.theglobeandmail.com/globe-drive/adventure/red-line/the-science-behind-winter-tires-and-how-they-work/article32531630/. [Accessed 5 May 2017].

[16] Bridgestone Tires, "Blizzak Winter Tire Technology: MultiCell Compound," 2011. [Online]. Available: https://www.youtube.com/watch?v=uQKnTcNXcDo. [Accessed May 25 2017].

[17] E. Cardile, "Resource.ansys.com," 2013. [Online]. Available: http://resource.ansys.com/staticassets/ANSYS/staticassets/resourcelibrary/article/AA-V7-I3-On-the-Fast-Track.pdf. [Accessed 5 Desember 2016].

[18] B. Finio, "Science Buddies," 2017. [Online]. Available: http://www.sciencebuddies.org/science-fair-projects/project_ideas/Physics_Springs_Tutorial.shtml. [Accessed 4 June 2017].

[19] efunda, "efunda," [Online]. Available: http://www.efunda.com/formulae/solid_mechanics/mat_mechanics/elastic_constants_E_nu.cfm. [Accessed 29 March 2017].

[20] ANSYS, Inc., "ASNYS Mechanical User's Guide," 2013, p. 883.

[21] P. Schatz, "Philschatz," [Online]. Available: http://philschatz.com/physics-book/contents/m42189.html. [Accessed 4 June 2017].

[22] Virtual racing school (VRS), 2017. [Online]. Available: https://virtualracingschool.com/academy/iracing-career-guide/setups/tyre-pressures-basics/. [Accessed 4 june 2017].

[23] Michelin, Director, *How the MICHELIN® X® Tweel® Airless Radial Tire Works.* [Film]. Michelin, 2015.

[24] Michelin, "Michelin.com," 2013. [Online]. Available: http://www.michelin.com/fre/innovation/domaines-d-intervention/innovation-pneu-et-alternatives/2004-Technologie-MICHELIN-TWEEL. [Accessed 5 December 2016].

[25] Bridgestone, "Bridgestone," [Online]. Available: http://www.bridgestonetire.com/tread-and-trend/tire-talk/airless-concept-tires. [Accessed 15 June 2017].

[26] R. Bell, "Geenville online," 2014. [Online]. Available: http://www.greenvilleonline.com/story/news/local/2014/11/20/michelin-executive-tweel-ready-passenger-car-market/70026218/. [Accessed 4 Desember 2016].

[27] CNET, "Youtube," 2014. [Online]. Available: https://www.youtube.com/watch?v=gkeTnS9e8_U. [Accessed 5 Desember 2016].

[28] N. Parke, "Astronotes," 2013. [Online]. Available: http://www.armaghplanet.com/blog/nasas-lunar-rover-everything-you-need-to-know.html. [Accessed 5 Desember 2016].

[29] H.-H. Lee, "Chapter 01. Introduction," in *Finite Element Simulations with ANSYS Workbench 16*, 2016.

[30] Photobucket, "Photobucket," 2013. [Online]. Available: http://photobucket.com/gallery/http://s1275.photobucket.com/user/Ultrasonic2/media/bfb9c26c-1a7e-49f1-a04f-2cccf9bf5d8c_zps020821e8.jpg.html. [Accessed 28 March 2017].

[31] F. Hauge, Interviewee, *Lufttrykk i vinterdekk.* [Interview]. 1 October 2016.

[32] Michelin, "Michelinman.com," 2017. [Online]. Available: http://www.michelinman.com/US/en/help/how-is-a-tire-made.html. [Accessed 10 May 2017].

[33] Marshal, "Marshaltyre," 2017. [Online]. Available: http://www.marshaltyre.co.uk/structure.php. [Accessed 1 05 2017].